5-2006

The Role of Novel Magnetic Interactions in Surface-Supported Magnetic Nanodot Assemblies

Maria Asuncion Torija Juana
University of Tennessee - Knoxville

To the Graduate Council:

I am submitting herewith a dissertation written by Maria Asuncion Torija Juana entitled "The Role of Novel Magnetic Interactions in Surface-Supported Magnetic Nanodot Assemblies." I have examined the final electronic copy of this dissertation for form and content and recommend that it be accepted in partial fulfillment of the requirements for the degree of Doctor of Philosophy, with a major in Physics.

E. Ward Plummer, Major Professor

We have read this dissertation and recommend its acceptance:

Jian Shen, Bin Hu, Hanno Weitering, Victor Barzykin

Accepted for the Council:
Dixie L. Thompson

Vice Provost and Dean of the Graduate School

(Original signatures are on file with official student records.)

To the Graduate Council:

I am submitting herewith a dissertation written by Maria Asuncion Torija Juana entitled "The Role of Novel Magnetic Interactions in Surface-Supported Magnetic Nanodot Assemblies." I have examined the final electronic copy of this dissertation for form and content and recommend that it be accepted in partial fulfillment of the requirements for the degree of Doctor of Philosophy, with a major in Physics.

E. Ward Plummer

Major Professor

We have read this dissertation and recommend its acceptance:

Jian Shen

Bin Hu

Hanno Weitering

Victor Barzykin

Accepted for the Council:

Anne Mayhew

Vice Chancellor and Dean of Graduate Studies

(Original signatures are on file with official student records)

The Role of Novel Magnetic Interactions in Surface-Supported Magnetic Nanodot Assemblies

A Dissertation Presented for the Doctor of Philosophy Degree

The University of Tennessee, Knoxville

Maria Asuncion Torija Juana

May 2006

DEDICATION

To my father, who taught me how to dream, to my mother who taught me how to make the dreams come true.

ACKNOWLEDGEMENTS

In all the rush to wrap up the thesis documents and set up the defense, I almost missed the most important part, to come back and smile remembering all the great people who made the thesis possible.

Firstly, I want to thank Jian Shen and Ward Plummer. The first meeting with both was in the fall of 1999, and I was so nervous trying to understand the words that the physics was almost secondary. Thanks to both, for giving me the opportunity in 1999 and for directing my thesis, but most importantly, thanks for their contagious and genuine excitement for physics. They mentored and encouraged me through all the steps in this dissertation.

I would like to acknowledge John Pierce for his unlimited patience, advice, and transportation to ORNL during my car-less phase.

Thanks to great people in ORNL and UT : John Wendenlken, Art Baddort, An Ping Li, Zhang Gai, and Gary Ownby. With their assistance, every leak found a solution.

During these four and a half years, I had he great pleasure to collaborate with many great people, Thanks to Dane for guidance with chamber set-up. Thanks to Jian Xian Ma for his knowledge in manganites. Thanks to Changan for the great opportunity to collaborate in the semi-conductor project, and the gift of his company in the lab. No Soung and Charles helped me out with the never ending cooling problems, and Wenchin, was a real pleasure as coworker and friend.

Thanks to Vickie Barnes, Vickie Chiocca and Maria Farwell, because their smiles and management of tedious bureaucracy and broken windows. I will miss the whole egg room, Honk, Min Hu, Von Braum, Jiandi, Ro b and TeYu . Good luck to Noppi with the chamber.

Writing was hard and difficult task without Vickie and Zach Ward. Thanks to Marianne Breignig for her guidance. And most special thanks to Hanno Weitering for his constant and dedicated support until the end.

Thanks to the following persons for motivation and passion for physics during my undergraduate years: Claudio Aroca and Elosia Lopez in Madrid and Jagadesh Moodera in Boston. I will never forget you.

The document would be impossible without the help of my friends. And here, I going to have problems to mention everybody. They have made Knoxville my home and thave been there in both the joyous and tough things. Maria Varela is a brilliant scientist, but her best attribute is her soul. I want thank her for her help, support, advise, and quality time with Mikey and Chloe. Thanks to Leon: because the Ph. D. process was not always easy or simple, but the final outcome is wonderful. Thanks for your support, Thanks to Eve, Klauss, Pia, Karen, Brian and Pedja, for the missed parties. Thanks to Doug and CJ for listening. Thanks to Idoia and Dr. B.A.Gelday. Thanks to Oscar and Perla for the birthdays. I wanr to thank my friends from Spain, for their company and their sense of humor.

A big part of me lives in Spain. My parents have dedicated their lives to my sisters and me. They have been great, even when I had difficulties. Thanks to my sisters,

Alicia and Irene, they kept me in a positive state every time I talked to them. And I cannot forget my aunt Rosario and my uncles Luis and Julian, who made this long trip possible.

This was a great fun. I would start all over again if I were four years younger.

ABSTRACT

The manipulation of matter at the atomic scales facilitates understanding of the fundamental properties of magnetism and opens the possibility of designing systems with novel magnetic properties with limitless industrial applications. This thesis seeks to identify nano-scale magnetic coupling mechanisms in nanostructures assemblies and to better understand different magnetic phases and the associated transitions. This was accomplished through the study of three prototype systems: Fe nanodots of controlled size and density on single crystal substrates of nonmagnetic metals, fractal – dimensional Fe on Cu(111), and FeGe nanowires on Ge(111). The first system shows the presence of a novel magnetic coupling in the nanodot arrays through the surface substrate, allowing the design of a Fe nanodot/Cu multilayer system with tunable magnetism in bulk and on surface. The second system shows a magnetic phase transition with unusual interface magnetism. The third shows how magnetic nature of FeGe (antiferromagnetic) can be shifted in nanostructures to ferromagnet under compressive strain. In all the topics, a new magnetic characteristic has been observed and discussed in details. The novel methods used to fabricate and control nanostructures will have a great impact in studying the emerging physical phenomena of magnetic materials in reduced dimensionality.

TABLE OF CONTENTS

LIST OF TABLES

LIST OF FIGURES

Chapter 1. Magnetism: From Large to Small

Experimental progress made in the last decade in growth and characterization techniques, has allowed us to obtain precision atomic distribution of nanostructures. This has enabled new applications in nanotechnology but more importantly, new science. The current availability of nanostructure systems whose morphology can be tailored almost at will, allows the study of emerging physical properties related to reduced dimensionality. Magnetism, one of the oldest scientific fields of study in nanostructure materials (nanomagnetism), has received a great deal of attention in recent years due to the new variety of phenomena observed. At nanometer scale, even the most fundamental magnetic properties, such as magnetic moment, magnetic coupling, magnetic anisotropy, and ordering temperature, can be dramatically different from those of the bulk.

As nanostructured materials challenge our understanding of magnetic interactions at the nanometer level, it is the main goal of this thesis to explore and understand new magnetic behaviors in artificially fabricated nanostructures. Ultimately, our findings may help to design new devices and applications (for storage, reading heads, etc) with specific, desired magnetic properties.

1.1 Historic development of magnetic research

From the beginning of civilization, mankind had awareness of magnetic materials. Magnetite was a common component in loadstone which was known by the Chinese and Greek civilizations as early as 800 BC [1-3]. The first documents about magnets often gave magnets a soul, divine components, or other magical properties which reflected the ancient myths, superstitions and legends of each culture.

Greek philosophers attempted the first explanations for the surprising phenomenon of rocks that could move iron. Thales of Mileto attributed them a soul, while Aristole pointed out that both rocks (magnetite and iron) share some kind of unity and that there ought to be some kind of intermediary to explain the action at a distance.

The Chinese civilization used lodestone as a primitive compass around 86 AC. They realized that a spoon-shaped loadstone floating in a bowl of water points towards the south. The first time that it was used, it helped to direct the Emperor's fertility ceremonies towards the south. This eventually lead to the compass. The compass has played a major role in the development of western civilization. Since the Europeans started using the compass in the sixteenth century, the ability to locate the direction to the North Magnetic Pole, allowed accurate long distance sea and ground navigation. Basically, the extended use of the compass made possible cultural exchange during the renaissance.

The actual understanding of magnetic phenomena started with an experimental observation by Oersted in 1820. During a lecture, he observed how a magnetic needle changed direction when placed near an electrical circuit. Subsequently, a great number of

experimentalists and theorists worked to establish the connection between electric and magnetic phenomena. In 1820, Ampere introduced the concept that internal electrical currents induce magnetism; Ampere's and Biot – Savart's Laws established the basis of electromagnetism. Faraday discovered electromagnetic induction and conceptualized the idea of magnetic field and force lines. Additionally, Faraday was responsible for the first explanation of magneto-optical phenomena.

A great milestone in the history of magnetism was the formulation of electromagnetic theory by Maxwell in 1873, who quantified the relationship between electric and magnetic field in his well-known Maxwell equations.

This, combined with the wave formulation done by Herzt two years later, became the basis for the electromagnetic revolution, which eventually led to electrification of the planet and global communications.

Despite these advances, magnetic materials still remained a mystery until the beginning of the Twentieth-century. Weiss was the first one to describe ferromagnetic materials at the microscopic level. He assumed that interactions between magnetic molecules could be understood as a molecular field. Combining this concept and the Lagevin theory for paramagnetic materials, the universal concept of ferromagnetism was qualitatively explained.

A paradox comes along when statistical physics is applied to magnetic materials, as already highlighted by Bohr's statement: 'the net magnetization vanishes at any temperature'. This conflict was solved by Quantum Theory. Bohr postulated that the angular momentum of an electron was quantified, and that orbital magnetic moments are

associated with the orbiting electron currents. Goudsmit and Uhlenbeck proved the existence of intrinsic spin angular moment in 1925. Its value was twice that expected by theory. Dirac explained this fact using a relativistic invariant in the Schrödinger equation.

Today, we understand magnetism as a sum of quantum and relativistic phenomena. Macroscopic magnetic order is a collective phenomena produced by the long range interaction amongst the individual magnetic moments inside a material. The molecular field, first proposed by Weiss, is in fact the sum of paramagnetic interactions between molecules or atoms with an intrinsic magnetic moment. Ferromagnetism is only one manifestation of these magnetic collective phenomena that also include ferrimagnetism and antiferromagnetism. In the last century, the introduction of quantum mechanics has allowed a more detailed classification of magnetic materials. This classification is sought now in terms of the electronic properties, metallic or insulating behavior, and of the nature of the magnetic moments, being related to the presence of localized or itinerant electrons [4].

The most common magnetic materials, like Fe or Co, are metals with itinerant magnetic moments. They are called band ferromagnets, because they have a narrow partially filled electric band which controls electrical conductivity as well as spontaneous magnetization. The mechanism responsible for this behavior is a many-body problem that is not well understood in certain cases.

Another interesting ferromagnetic material is the insulating ferromagnet, which has localized magnetic moments. The Heisenberg model describes this ferromagnetism:

$$H = -\sum_{i,j} J_{ij} S_i \bullet S_j$$

J is the exchange coupling constant between magnetic moments, S. The exchange between magnetic moments can be direct, as in cases of Eu based compounds where the magnetic moment is originated in the 3d or 4f, 5f shells. On the other hand, in cases like MnO the distance between magnetic moments doesn't allow direct exchange, but there is an indirect coupling between the magnetic ion s through the O^{2-} ions.

Other metals, such as Gd, have localized magnetic moments in the hybrid level s-f. The indirect coupling between the magnetic moments is due to the spin polarization of the conduction electrons: it is the Ruderman-Kittel-Kasuya-Yosida (RKKY) interaction.

Also, there are a group of antiferromagnetic oxides that (best example is NiO), follow the Mott-Hubbard model. The band structure revealed by photoemission shows the two different 3d-character bands for Ni with two fully occupied, and another empty, separated by the insulating gap. The magnetic behavior comes form the broad inner states, and so is called itinerant, but the material is an insulator.

1.2. The Attraction of Magnets at the Nanometer Scale

The exchange length is defined as the upper limit of magnetic moment interactions. This characteristic length depends on the type of interactions present and is generally in the nanoscale order. If this length is comparable with the system size, the physics of the system will likely be very different from the magnetic bulk phenomena. In addition, when reducing system size, the presence of interfaces will increasingly dominate the system properties, because the surface-to-bulk ratio grows. Spatial

confinement is also important, because it determines the correlation effects in spin phenomena. (i.e. Spin wave wavelengths are intimately linked to the dimensions of the material [5]). Moreover, new quantum phenomena become observable as many parameters don't have continuous spectra any more, but are quantized instead.

The best example to demonstrate the effect of spatial confinement is the discovery of giant magnetoresistance (GMR) in multilayers structures. These multilayer structures typically consist on ultrathin ferromagnetic layers that are separated by nonmagnetic spacer layers. This coupling can be ferro- or antiferromagnetic and is determined by the thickness of the spacer layer. In these magnetically coupled multilayers, the GMR effect consists of a large change in the electrical resistance under the influence of a magnetic field. A simple device illustrating this effect is a magnetic-nonmagnetic-magnetic sandwich structure of layers epitaxially grown on top of each other, such as Co/Cu/Co hetero-structures. Both magnetic Co and nonmagnetic Cu contain electrons with opposite spin directions, 'spin up' and 'spin down'. In the case of the Co, the number of electrons with spin up and spin down is not the same, but this is not the case in Cu. When a voltage is applied to the Co/Cu/Co heterostructure, the spin up and spin down electrons will try to move from one electrode to the other. The spin up electrons of the Co have matching potential with the Cu. Thus, the spin up electrons will pass easily through the first interface, while the spin down electrons with lower potential will be mostly scattered at the interface. In the second interface, the Co up electrons can only pass if there is 'empty space' available. This empty space is created only if the magnetization of both Co layers is parallel. The result is a minimum resistance when both Co layers have parallel

magnetizations and a maximum value when the magnetizations are opposing each other. This change in resistance is the so-called GMR, which is usually around 10-100%, two orders of magnitude higher than in regular materials [5].

The GMR is a clear example of a new phenomenon achieved by reducing the dimensionality. In a GMR device, the relevant magnitude or characteristic length is the spin diffusion length, or how far the electron can travel without losing its spin orientation. In metals, it can be around 10-50 nm. So if the layer thickness is lower than this value, it is possible to guarantee that the electrons will keep their coherent orientation across the next layer.

Finally, it is worth mentioning that one of the most anticipated prospects in nanomagnetism relies on its applications to Quantum Computing. During the last few years, quantum computation has been advertised in the same way as cold fusion or room temperature superconductivity: a great theoretical idealization whose materialization lies far in the future. Quantum computing is making remarkable progress. The basic premise is that the information unit, the quantum bit (q-bit), will not store a zero/one value. The q-bit will be a quantum state, which would store more like a density of probability. Mathematically, operations in a quantum computer will solve problems that the traditional binary computer would take and infinite time to solve. To obtain the information unit, it is necessary to control the system to the quantum level for period of time enough to be able to write and read the q-bits.

1.3 Nanomagnetism: What has been and what needs to be known

1.3.1 The current status

As mentioned earlier, confining the spatial dimension of magnetic material smaller than the ferromagnetic exchange length can fundamentally change its magnetic behavior. In fact, some of the underlying ideas considerably predate current research activity. For example, when Bloch introduced the concept of spin waves in 1930, he already recognized that a two-dimensional (2D) spin system with Heisenberg interactions couldn't be ferromagnetic at finite temperatures. This was later on proved by Mermin and Wagner elegantly using a renormalization group theory, which shows that no phase transition can occur in two- and one- dimensional (1D) Heisenberg system [7]. In the early 1980s, developments in ultrathin film growth, in-situ magnetic characterization, and additional experimental results in 2D systems, further demonstrated the existence of ferromagnetic order. Although the phase transitions tend to occur at lower temperatures than the bulk Curie temperature and are often somewhat smeared due to the finite size-effect, these results did raise doubt of the validity of the Mermin-Wagner theorem in experimental systems. This dilemma was solved brilliantly by Bander and Mills, who explained [8] that magnetic anisotropy and long range dipolar interaction in ultrathin films can suppress the spin fluctuations in a 2D Heisenberg system and lead to a true long range order. Subsequently, many more interesting magnetic properties have been discovered and explained in 2D systems. These include enhanced magnetic anisotropy due to broken symmetry, reduced ordering temperature due to finite-size scaling,

enhanced magnetic moment owing to the band narrowing, and changed universality class due to reduced dimensionality.

Just when the studies of the 2D systems reached their peak, major breakthroughs were made in the study of 1D systems occurred, thanks to the development of the step-flow growth method. Quasi one-dimensional stripe arrays of Fe have been grown on both W (110) and Cu (111) substrates and magnetically characterized in-situ [9]. The initial results were rather confusing, as the Fe/W stripes showed ferromagnetic behavior and the Fe/Cu stripes showed paramagnetic behavior [10]. It was later understood that the ferromagnetism in the Fe/W stripes originated from the strong ferromagnetic dipolar interaction. A striking observation related to 1D stripe is the domain configuration, which has an atomically abrupt domain wall according to images taken from spin polarized STM. Very recently, single atomic chain of Co atoms have been prepared on Pt (997) substrate and the spin axis of these Co atoms was observed to be at a canted angle from the surface normal [11].

Compared with 2D and 1D systems, the 0D nano-particles have been investigated with a much longer history. The equilibrium of non-interacting single-domain particles at non-zero temperatures is generally described by well-established superparamagnetic theory[12-16]. Under this theory, the magnetic moments within each magnetic particle move coherently and can be treated as a single giant moment. The giant magnetic moment is coupled to magnetic anisotropy, which provides several equivalent equilibrium states, depending on the actual type of the anisotropy. For an assembly of these kinds of particles, the giant moments will have a balanced distribution in those

equivalent states, leaving zero net magnetization of the system. An important concept associated with superparamagnetism is the blocking temperature, below which the thermal energy is not large enough to flip the giant moment within the measuring time. The particles can be considered as ferromagnetic particles below the blocking temperature, which is determined by the competition between the magnetic anisotropy barrier and thermal activation.

One of the characteristic features of a 0D particle is its large surface to volume ratio. It has been speculated that the large surface to volume ratio would give rise to enhanced magnetic moment and anisotropy. Early experiments on isolated Fe [17] and Co[18] particles embedded in nonmagnetic metals, indicated only small changes of 0K saturation magnetization as a function of particle size. The measured results, however, are not necessarily connected with the intrinsic properties of 0D free clusters, since the electronic hybridization at the particle/host interface could largely affect the surface magnetic moment. In the 1990s there was growing interest in the re-examining the magnetic moment of 0D clusters. These are free clusters made by cluster beam sources, and their magnetic moments were measured by a conventional Stern Gerlach apparatus. Enhanced magnetic moments were reported for Fe [18], Co[19], and Ni[20] free clusters, which typically contain several tens to several hundred atoms. Even Rh [21], which is nonmagnetic in bulk, exhibits a sizable moment in cluster form. In most cases, the magnetic moment oscillates with the number of atoms contained in the cluster, reaching maxima or minima for open or closed geometrical shell, respectively. Since the open and closed shells represent the largest and the smallest surface volume ratio, respectively, this

is a clear demonstration of the significance of the surface effect on moment enhancement [22].

While the fundamental 0D magnetic behavior can be addressed in studying the magnetic properties of isolated particles or free clusters, magnetic dot arrays attract the most attention due to their potential application in high density recording media. Various methods have been introduced to study the magnetization reversal process of the arrayed particles under external field and changing temperature[23-24]. When the dot arrays are dense enough, the interaction between the dots appears to have influence on the magnetic properties. For example, the simplest dipolar interaction was found to increase the blocking temperature by effectively increasing the energy barrier between adjacent low energy states [25-26].

1.3.2 Hot topics in nanomagnetism research

A. Interacting magnetic nanostructures.

Most of the recent advances in nanomagnetism have been made in laterally structured thin films. There are two different general type of growth: film patterning by lithography and the use of nanostructured substrates.

In film patterning by lithography, studies of sub-micron permalloy dots [27-30] by Cowburn and Welland showed the versatility of the collective magnetism controlled by interactions, where a synthetic antiferromagnetic order can be generated by elliptical dots. Dipolar interaction was also observed in the collective switching of iron square-shape dots.

Self-assembled systems are helped by the natural characteristic of the substrates. There are several interesting examples of magnetic coupling effects. For example, the already mentioned studied of Elmers [9] on Fe stripes on W(1000). The transition to ferromagnetism is driven by the dipolar interaction between wires.

In this thesis a novel growth method, Buffer Layer Assisted growth, is used to produce arrays of magnetic nanodots on a metal substrate. Despite the predicted paramagnetic behavior, they show a collective strong ferromagnetism. Studies of dipolar interaction, anisotropy and surfaces influences, indicate the presence of a novel magnetic interaction driven by the surface states of the non magnetic substrate.

In vertical nanostrucures, dipolar coupling and pinning of the domain walls is reponsible for many effects in Magnetic Tunnel Junctions (MTJ). A most interesting phenomena is oscillatory exchange coupling RKKY [31-33].As the thickness of the spacer layer varies between two ferromagnets, the coupling can oscillate in sign, and generally, it dominates a small spacer thickness. Shortly after GMR was discovered in Fe/Cr multilayers [34] coupling between Fe, Ni, or Co was shown as a common general feature[35]. RKKY was first observed within magnetic impurities in metals [36] where spin polarized disturbances, (interfaces in multilayers and impurities in the metals) are coupled by the influence of the electron in the metal or host.

From the analytical expression of RKKY in 2D systems, and considering that it only occurs along the axis of growth, it is possible to deduce that the coupling oscillates with a period of half of the Fermi wavelength ($\lambda_F/2$). Experimental disagreements [37] induced deeper refinement in the theory. Bruno and Chappert [38-39]introduced the

critical spanning vector of the Fermi surface, vectors that connect the two identical Fermi surface points, as origin of the oscillations. Then, the coupling strength depends on $1/t^2$ (t is the interlayer thickness). Comparing with magnetic impurities in a metal matrix, the strength is $1/d^3$ (distance between impurities). A direct consequence is that the RKKY effect weakens in a 3D system faster than in a 2D array.

Interactions and dimensionality dependence of the system are discussed in the second paper of the thesis. The previously mentioned nanodot array is the magnetic layer unit in a multilayer system (spaced by Cu layers). The surface of the system (2D array) demonstrate the forementioned ferromagnetism, but the bulk forms a spin glass due to dipolar and RKKY interaction in random anisotropy clusters. This system is remarkable because it allows the possibility to distinguish surface from bulk magnetism.

B. Phase transition.

In nonoscale growth, materials initially grow epitaxially with the substrate. If there is a mismatch, initial layers grow with strain in a metastable equilibrium until a critical thickness where the material relaxes and adopts the bulk lattice parameter. These meta-stable phases can have very different and interesting properties from the bulk. In addition to the structural transitions, magnetic materials can have a magnetic transition. The natural tendency of individual atoms on a surface is to have perpendicular anisotropy to this surface, but with the increase in thickness, the orientation of the easy axis lies in a plane. There are many cases in which both transformations are linked and magnetism drives the structural transition, as demonstrated in Fe on Cu [10] or L0 allyos [40].

The interplay between the structural and the magnetic phase transitions often lead to some kind of nonuniform magnetic states during the phase transition process. Identifying the coexisted structural and magnetic phases is crucial for understanding the nature of the phase transition in surface-supported nanostructures. These phases can coexist both in the lateral and the vertical directions with respect to the substrate normal. The distribution of the lateral phases is best resolved by high resolution magnetic imaging techniques such as scanning electron microscope with spin polarization analysis (SEMPA) and spin polarized scanning tunneling microscope (SP-STM). For the vertical phases, however, there have been no good ways to characterize them, which strongly hinders the understanding of the phase transition.

In chapter 5, we discuss our approach to solve this problem. We use low-temperature (~ 65 K) grown Fe on Cu(111) as a prototype system to demonstrate that it is indeed possible to resolve the vertical phases using the combination of STM and magneto-optical Kerr effect. Interestingly, at low temperatures Fe grows on Cu(111) as fractal-dimensional islands. With increasing nominal thickness, the fractal islands undergo a low-spin to high-spin magnetic phase transition and a perpendicular to in-plane spin reorientation transition. In-situ magneto-optical Kerr effect studies reveals the existence of highly nonuniform magnetization distribution along the surface normal. With the help of morphological layer distribution data obtained by STM, we are able to map out the magnetic phases along the surface normal. The origin of the magnetic phase transitions and its nonuniformity are attributed to a nonuniform structural phase transition from face centered cubic (fcc) to body centered cubic (bcc). As a matter of fact, part of the Fe at the Fe-Cu interface has never made to the bcc (high-spin) state after being frozen at the interface.

C. Spintronics.

In this vibrant field, it is possible to point out some of the many paths being studied. Industry and science have a common interest in a device that can provide spin injection. The search for high magnetirresistance has driven the design and the theory of multilayer systems. New and interesting materials like complex oxides LSMo/ STO/LSMO [41] and half metallic as electrodes [42] are available to researchers..

The implement of any of these devices requires conexion with a semiconductor in some point. That is the power reason behind the search for a magnetic semiconductor that would eliminate the step. Much Attention has been given to doping a regular semiconductor with magnetic impurities [43] It is thought that exchange interactions between electronic band states and local moments enhance the spin splitting in holes. For bidimensional systems, it has been possible to create a two-dimensional electron gas, where the populations of electrons interact ferromagnetically with local moments.[44] .

Apeendix 2 explores a different approach to semiconductor-ferromagnet combinations. A bulk antiferromagnet, FeGe is presented in a new configuration: FeGe nanowires. These nanowires are actually ferromagnetic when epitaxially grown on Ge (111). This change is attributed to the structural effects of epitaxial strain in the nanostrucure that alters the genuine magnetic ground state.

Chapter 2: Magnetism and Magnetic Materials

2.1 Magnetic materials

This chapter examines the concepts, materials, growth methods, and characterization techniques used in this work.

We shall begin with a discussion of the microscopic origin of magnetism. The electron magnetic moment comes from the combination of electron spin and the orbital moment. Atomic magnetic moment is the total superposition of all of the spins in an atom. Magnetization is the net magnetic moment per unit volume. The response of an atom to a magnetic field can be diamagnetic or paramagnetic. In the diamagnetic case, the atoms do not have a net magnetic moment, and the response to an external magnetic field is a negative magnetization that cancels out the field inside the material. In a sense, the material shields the external field. Paramagnetism is found in materials whose atoms show an intrinsic non-zero magnetic moment. When a magnetic field is applied, the magnetic moments line up in the direction of the field, creating a positive magnetization.

Interesting magnetic properties arise when spin-spin interactions in solids lead to an ordering that can be characterized by an antiferromagnetic, ferrimagnetic, or ferromagnetic alignment [3]. In antiferromagnets**,** magnetic interactions favor antiparallel orientation of neighboring moments for temperatures below the Neel temperature (T_N). Above T_N the order disappears due to thermal fluctuations. Another way of looking at antiferromagnetic ordering, is to imagine two identical and interpenetrated spin sub-lattices with opposite orientations. The macroscopic net magnetic moment therefore

vanishes. On the other hand, ferrimagnetic materials consist of an antiferromagnetic lattice where the alternating antiparallel spins have different magnitudes. In this case, the macroscopic net magnetic moment is non-zero, even in the absence of an external field. For ferromagnetism**,** interactions between moments provoke a parallel alignment of adjacent spins, which gives rise to a non-zero spontaneous magnetization in the absence of an external field.

2.2 Macroscopic magnetism

In many magnetic materials, the macroscopically observed ground state does not reflect the alignment in the atomic configuration, due to domain formation. A domain is a region of the material within which the intrinsic order (ferro, antiferro or ferri) is preserved, but it is not necessarily coherent between domains. Domain walls are regions where the spins do not follow the magnetic order. Although magnetic moments within each domain are ferromagnetically aligned, the orientation of the magnetization is different from domain to domain. A schematic representation of domain structure is shown in Fig. 2.1.

2.2.1 Hysteresis

A common effect in ferromagnets is hysteretic behavior (shown in Fig. 2.1). Applying an external magnetic field makes the spins align with each other until the magnetization saturates. When the external field is removed, the magnetization remains finite at a value M_1, which is known as the remnant magnetization. The magnetization

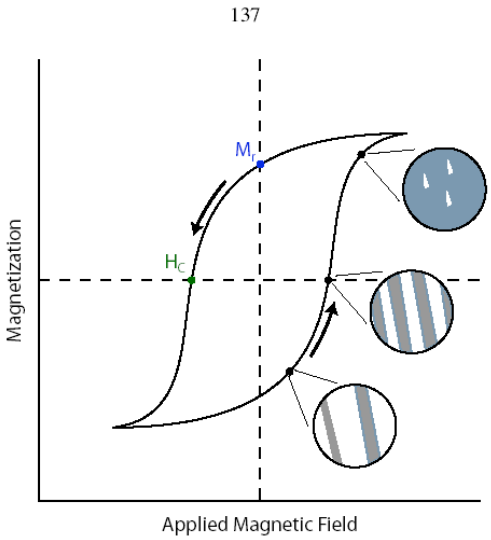

Figure 2.1 Magnetic Hysteresis Loop

The insets, contain a schematic of the domain distributions.

can be decreased to zero by applying an external field H_C (coercive field) in the opposite direction. The study of demagnetization processes can explain how a material is magnetically constituted at the atomic level in addition to relevant information about the domain wall dynamics.

2.3 Nano scale Effects: monodomain structures

The domain formation requires that some spins not follow the natural tendency of the material (ferro, antiferro, or ferromagnetic), consequently, there is an increase in local energy. If the material is small enough, the reduction in overall energy does not compensate domain formation energy, and the system remains monodomain. Monodomain particles in ferromagnetic materials behave as unified spins with high magnetic moments. In antiferromagnetic materials, a monodomain particle will have uncompensated spins on the surface. Thus, particles formed by antiferromagnetic materials will have a net magnetic moment.

Over the last few decades, the study of arrays of monodomain particles has been very prolific. Two different categories can be considered: weak and strongly interacting particles. Thermodynamic perturbation theory has been applied successfully to the weakly interacting particles, while the strong interaction requires nonequilibrium dynamics. In both cases, the Hamiltonian aspects will gain contributions from the magnetic anisotropy, the interaction of the particle, the external field, and the dipole-dipole interaction.

2.3.1 Anisotropy

Magnetic anisotropy determines the angular dependency of the internal energy and direction of the spontaneous magnetization. The easy (hard) axis is defined as the direction that requires the lowest (highest) field to saturate the magnetic moments. Bulk materials exhibit magnetocrystalline anisotropy, originating from the spin-orbit coupling and the crystal structure. The magnetic crystal anisotropy will have the crystal's symmetry, but in monodomain particles, it is sometimes possible to simplify the dependency to uniaxial anisotropy:

$$E_a^{uni} = K_1 V \sin^2\theta + K_2 V \sin^4\theta + ...$$

where V is the volume of the particle, K_1 and K_2 are anisotropy constants, and θ is the angle between the magnetic moment and the symmetry axis.

The most intuitive anisotropy origin is shape anisotropy, which derives from magnetostatic energy. For simple shapes, mathematical calculations are possible, i.e. the ellipsoid of revolution is given as:

$$E_{m-ellipsoid} = \frac{1}{2}\mu_0 V M_S^2 (N_Z \cos^2\theta + N_X \sin^2\theta)$$

where θ is the angle between the magnetic moment and the Z polar axis. Ms is the saturation magnetization, and $N_{x,y,z,}$ are the demagnetization factors. For ellipsoids and uniaxial magnetic anisotropy, it is possible to rewrite the anisotropy (to first order) as:

$$E = -A\cos^2(\theta)$$

where A=KV is the anisotropy energy barrier. In nanoparticles, the reduction of the different anisotropies to basic uniaxial anisotropy can supply all the basic elements necessary to study the system.

2.3.2. Superparamagnetism

The dominant behavior observed in ferromagnetic nanodot assemblies is called superparamagnetism [2]. Assuming uniaxial anisotropy of monodomain individual particles, the anisotropy energy creates two potential wells separated by an energy barrier, A. The magnetic particles are assumed to have a Brownian-type rotation, in which the thermal fluctuations affect the time for the rotation over the barrier, τ. This decay constant can be approximated by an Arrhenius form:

$$\tau \cong \tau_0 \exp(\beta A)$$

In general τ_0 is of the order of 10^{-10} or 10^{-12} seconds, and in order to observe macroscopic magnetization, the exponent should have a value greater than 25 (τ_{0bs} =100sec). When observation time is much longer than the relaxation time, the magnetism of the system has the same moment distribution as a paramagnetic system. As the particle magnetic moment is larger than a single spin, the behavior is called

superparamagnetism. If the observation time is lower than the relaxation time, the magnetic moment is blocked in a potential well in a state of stable bulk magnetization. If both time parameters, observation and relaxation, are comparable, dynamical effects will be observed. In the thermodynamic landscape, it is possible to introduce the Hamiltonian for a non-interacting nanoparticle:

$$H = -\frac{A}{m^2}(\vec{m} \bullet \vec{n})^2 - \mu_0 \vec{m} \bullet \vec{H}$$

$m=M_sV$ is the magnetic moment. The First term referring to the anisotropy, A is the previously mention anistotropy energy barrier, and n is the vector along the anisotropy axis. The second term is the interaction with the external field. It is possible to study the Hamiltonian in the dimensionaless form:

$$-\beta \mathrm{H} = -\sigma(\vec{s} \bullet \vec{n})^2 - \xi(\vec{s} \bullet \vec{h})$$

where $\sigma=\beta A$, and $\xi=\beta\mu_0 mH$.

The Hamiltonian will be modified by the interactions. If the dipolar interaction is small compared with the anisotropy energy, there will be a new term in the Hamiltonian:

$$\vec{H}_i = \frac{m}{4\pi a^3} \sum_i G_{ij} \cdot \vec{s}_j$$

where the dipolar field in the particle is created by all other spins $_i$ and positions r_i. with the mean volume a^3.

The transverse component will be included in the adimensional Hamiltonian:

$$-\beta H = \sigma \sum_i (\vec{s}_i \bullet \vec{n}_i)^2 + \xi \sum_i (\vec{s}_i \bullet \vec{h}) + \xi_d \sum_{i>j} \omega_{ij}$$

where $\zeta_d = \frac{\mu_0 m^2}{4\pi a^3} \frac{1}{k_B T}$ and $\omega_{ij} = \vec{s}_i \cdot G_{ij} \cdot \vec{s}_j$

If the dipolar energy (the last term) is small, the solution for the Hamiltonian can be treated as an extra harmonic term. The rotational movement will have 'damping' effects. This means that the relaxation processes will slow down. The presence of a weak interaction would be equivalent to increasing the energy barrier of the anisotropy.

$$\tau \cong \tau_0 (1 - \frac{T}{T_g})^{-z\nu}$$

One effect that can broaden the distribution of the relaxation times is the size distribution within the array, because the decay would be different.

There are additional dot-dot interactions that can affect the system. [4,2]. This indirect exchange consists of the magnetic polarization of orbitals, or energy levels that originally are not magnetic. A possible case is interaction through the conduction electrons. Around the magnetic moment, the conduction electron spins can be polarized; and under the right conditions, a continuous wave of regions with opposite polarizations can be found. Such a system will be antiferromagnetic or ferromagnetic, depending on the distance between magnetic moments (in phase or antiphase). They can be

characterized by the RKKY interaction. The exchange constant between the magnetic impurities embedded in a metal follows the oscillatory law:

$$J(r) = J_0 \frac{\cos(2k_F r + \varphi_0)}{(k_F r)^3}$$

where K_F is the Fermi vector of the host metal, and J_0 and φ_0 are constants. This interaction is isotropic, but in some cases, anisotropic effects come from the anisotropy itself and other interactions.

Other classical interactions can appear in nanodot arrays, such as magnetic Casimir forces [5] and magnetic coupling by tunneling electrons [6]. The Casimir force is very weak and arises from zero-point quantum fluctuations when magnetic order changes. The coupling mediated by the tunneling electron is important when the tunnel barrier is small. It has been reported as the origin of room temperature ferromagnetism in Fe dots on an insulating CaF_2 / Si (111) substrate [7].

2.3.2. Spin Glass Material and Cluster Glass Arrays

Dense monoparticle arrays can show glassy dynamics due to strong dipolar interactions. Spatial disorder and random orientations of the anisotropy in the particles can induce disorder and frustration. With increasing particle concentration, the magnetic behavior may evolve from superparamagnetic to spin-glass like at the so-called glass temperature T_g. For T <Tg, there is a crossover between critical dynamics in short time scales and activated dynamics over long time scales. .

A real space model that can be used to study the crossover is the droplet model. It is based on three general concepts: chaos with temperature, domain growth and overlap length. Chaos with temperature means that small temperature changes can alter the equilibrium configuration of the magnetic moments completely on sufficiently long length scales. The length scale up to which no essential change in configuration is observed after a temperature step ΔT is called overlap length. At each temperature, the equilibrium spin glass state is formed by a ground state, plus thermally activated droplet excitations of various sizes. Droplets are low-energy clusters of spin with volume L^d and a fractal surface L^{ds}. The magnetization of the system is due to the polarization of the droplets. The typical droplet size after a time **tw** at constant temperature T is:

$$R(T,T_W) \propto \left(\frac{T \ln(t_w/\tau)}{\Delta(T)} \right)^{1/\Psi}$$

τ is the relaxation time. ΔT is the energy free scale, and Ψ is a barrier exponent. t_w is the waiting time at that field and temperature. For individual particles, the relaxation time is given by Arrhenius's law. All systems have an unavoidable size distribution. The time relaxation will have a distribution as well, and due to the exponential factor, the distribution will be broader than the anisotropy energy barriers.

In the droplet model, there are two spin configurations: Ψ and its counterpart. If the system is quenched at temperature $t_1 (<T_g)$, the spins will randomly belong to one of two configurations. The subsequent equilibrium process will be governed by droplet excitations that induce the domain growth to a typical length scale depending on t_w.

After this time, the fractal structures will equilibrate, but longer length scales than R will persist. If the system is quenched to a lower temperature T_2, the domain structure of T_1 still fits on scales smaller than the overlap length $l(T_1\text{-}T_2)$. After that, the domain growth at T_2 will begin and increase with waiting time. If the system comes back to T_1, the second fractal domain introduces a second dispersed domain structure. The system has memory of the magnetic history. This means that when the system comes back to T_1, and the magnetization pattern reflects the past T_1, the field, and the waiting temperature. Aging phenomena can reveal the structure of spin glasses. Detailed analysis of the memory effect might offer information about these interactions.

2.4 Characterization techniques

In most cases, if the nanostructure array is exposed to air, its intrinsic properties will be immediately affected. Therefore, a comprehensive characterization of these phenomena needs to be carried out *in-situ.* For this purpose, ultra high vacuum techniques are required. The two main in-situ characterization techniques used are Magneto-Optical Kerr Effect (MOKE) [8] and Scanning Tunneling Microscopy (STM) [9].

2.4.1 MOKE

The MOKE effect has made a tremendous impact on technology, due its use in recording magnetic media, MO disks, in old computers. In the last 20 years, the Surface Magneto Optical Kerr effect has become an indispensable tool to detect magnetism,

because its sensitivity allows the detection of magnetic materials under the monolayer regime.

The basic explanation for the magneto-optical effect is the intimate relationship between the electrons of the magnetized solids and photons. The microscopic origin of the magneto-optical effect is connected with the Lorentz force that electrons in the magnetized solid induce in the photons reflected from the sample.

The polarization of the light changes its ellipticity after being reflected in a magnetic material. The proper setup can register this change as proportional to magnetization in the material.

2.4.2. STM

Scanning Tunneling Microscopy (STM) [28] has been one of the most important techniques in the study of nanostructures. It is routinely capable of 1-0.1nm resolution in the vertical direction and can easily image structures whose lateral resolution is on the nanometer scale. To map the surface, the STM measures the current between the sharp metallic tip and the sample. At small distances, this tunnel current is exponentially dependent on the distance between the tip and the sample. The tip is precisely scanned over the surface by piezoelectric materials that change length with voltage. There are several possible modes to operate the microscope. In the 'constant height mode' the tip-sample distance is fixed, and the instrument records the variations in the current. In the 'constant current mode', the voltage applied on the piezo scanner is constantly changed

by feedback loop in order to maintain the same tunneling current. Use of STM is only possible with semiconductor or a conductor samples.

Chapter 3: Ferromagnetic Stability in Fe Nanodot Assemblies on Cu(111) Induced by Indirect Coupling through the Substrate

This Chapter examines the magnetic phenomena observed in Fe nanodot assemblies on Cu(111), a novel system with high stable remanent magnetization. A series of experiments were performed to determine the importance of the dipolar interaction and anisotropy. We also sought to elucidate the presence of a new magnetic interaction through the surface that stabilized system magnetism at high temperatures. My contribution is center in the magnetic measurements. It has been published in Physical Review Letter, vol. 2, num 23, 237201 (2004).

J. P. Pierce, [1,2] M. A. Torija,[1,2] Z. Gai ,[1,3] Junren Shi,[1] T. C. Schulthess,[4] G. A. Farnan, [1] J. F. Wendelken,[1] E. W. Plummer, [1,2] and J. Shen[1],* 1Condensed Matter Sciences Division, Oak Ridge National Laboratory, Oak Ridge, Tennessee 37831, USA

2Department of Physics and Astronomy, The University of Tennessee, Knoxville, Tennessee 37996, USA

3Department of Physics & State Key Laboratory for Mesoscopic Physics, Peking University, Beijing 100080, People's Republic of China 4Computational Sciences and Engineering Division, Oak Ridge National Laboratory, Oak Ridge, Tennessee 37831, USA (Received 23 February 2004; published 9 June 2004)

We report collective ferromagnetic behavior with high Curie temperatures (Tc) in Fe dot assemblies supported by the Cu(111) surface. Our ability to tune the average size and spacing of the individual dots allows us to conclude that enhanced magnetic anisotropy cannot account for this high-Tc ferromagnetic order. Because our Monte Carlo simulations have ruled out the dipolar interaction as the dominant factor in this system, we attribute the origin of the ferromagnetic order to indirect exchange coupling via the Cu(111) substrate.

To first order, assemblies of nanoscale magnetic dots are superparamagnetic. In these systems, thermal energy, which causes fluctuation of the dots' magnetic moments, becomes significant enough to overcome the anisotropy energy barrier and randomize their orientation at the socalled blocking temperature. This typically occurs far below room temperature. In real nanodot assemblies, it has been generally recognized that the magnetic dipoledipole interaction can affect the barrier height for flipping the spin of each individual dot as well as the collective magnetic behavior of the dot assembly [1–9]. Recently, in a Cu(100) surface-supported Co island assembly, longrange ferromagnetic order with a Curie temperature (Tc) of about 200 K was observed when the Co islands approached the limit of two-dimensional morphological percolation [10]. The observed ferromagnetic long-range order was interpreted as a consequence of the long-range dipolar interaction [11].

In this Letter, we report collective ferromagnetic behavior in two-dimensional Fe dot assemblies on the Cu(111) surface that persists above room temperature. Our ability to tune the average size and spacing of the dots enables us to investigate the relative

contributions of the mechanisms that support this unexpectedly robust magnetic order. Our experimental results and simulations indicate that the high-Tc ferromagnetism cannot be explained by either magnetic anisotropy or the simple dipolar interaction. Therefore, the ferromagnetic order in the Fe dot assemblies is a result of an indirect exchange interaction via the Cu(111) substrate.

Direct deposition of Fe onto Cu(111) does not lead to dot formation [12–14]. Therefore, the Fe/Cu(111) dot assemblies were synthesized by a novel method known as buffer layer assisted growth (BLAG) [15] in an ultrahigh vacuum (UHV) system with base pressures below 1 x 10^{-10} Torr. The Cu(111) single crystal surface was prepared by cycles of 1 keV Ne ion sputtering and annealing to 800 K, before it was cooled to about 15 K. Inert Xe gas of 5N purity was then released into the UHV chamber. Xenon exposures ranged from 0 to 600 L [1 langmuir (L)=10^{-6} Torr s]. Iron was then evaporated from a wire (5N purity) that was heated by electron bombardment. The deposition rate was independently calibrated by a combination of in situ scanning tunneling microscopy (STM), reflection high energy electron diffraction, and Auger electron spectroscopy. After Fe deposition, the sample was slowly warmed to 300 K to desorb the Xe buffer layer and allow the Fe dots to land on the Cu substrate. In situ STM and magneto-optical Kerr effect (MOKE) measurements were then performed.

Fe/Cu(111) dots grown by the BLAG method are shaped like slightly flattened hemispheres with a rather random spatial distribution. Figure 3.1(a) shows the STM morphology of a typical Fe dot assembly formed by depositing the equivalent of 0.8 ML (monolayer) Fe (nominal thickness) assisted by 200 L Xe. The density of the dots, after a

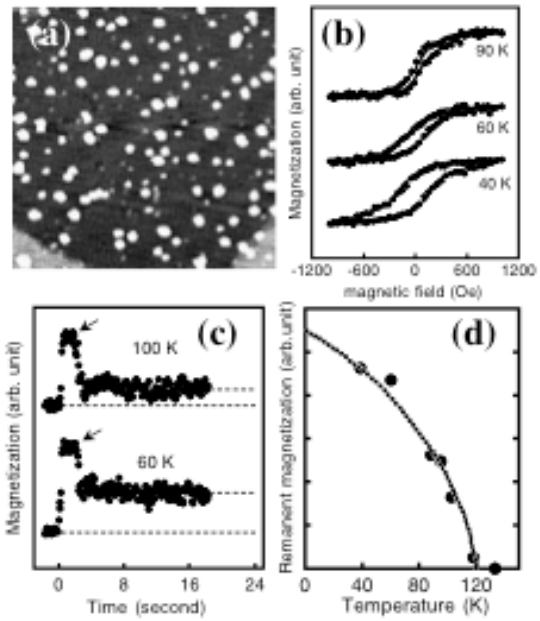

Figure 3.1 Morphological and magnetic characterization of typical array

Xe exposure of 200 L in 2(a), and as a function of Xe exposure at a fixed dosage of 1 ML in 2(b). Apparently, changing the Xe exposure has a more dramatic affect on the dot size and density than varying the Fe dosage. The fact that the dot size increases with increasing Xe exposure can be understood to result from the enhanced likelihood for Fe clusters to collide and stick to each other as they work their way toward the Cu surface through a (a) STM morphology (100 nm x 100 nm) of an Fe dot assembly on Cu(111) prepared with 0.8 ML Fe and 200 L Xe. (b) MOKE hysteresis loops of the Fe dot assembly at various temperatures. (c) Time dependence of the magnetization of the Fe dot assembly. An in-plane external field was applied at time ‘‘zero’’ and was switched off at the points in time indicated by the arrows. (d) Remanent magnetization of the Fe dot assembly as a function of temperature. The critical temperature is around 120 K.

statistical analysis of images taken at various areas on the surface, is estimated to be about 8.05 x $10^{3}/\mu m^{2}$. This yields an average dot volume of around $8.2nm^{3}$, i.e., ~700 Fe atoms if we assume a bcc structure. Dot profile analysis indicates that the average height and the average width of the Fe dots are 1.4 and 3.5 nm, respectively [16].

The MOKE measurements of the Fe dot assembly shown in Fig. 3.1(a) reveal clear ferromagnetic behavior. Figure 3.1(b) shows in-plane hysteresis loops of the dot assembly at various temperatures. No perpendicular magnetization can be measured even at maximal field of 2400 Oe, indicating that the Fe dots have an in-plane easy magnetization axis. The remanent magnetization (Mr) of the dot assembly, while strongly dependent on temperature, is remarkably stable with respect to time, as shown in Fig. 3.1(c). For the time-dependent magnetization measurements, the dot assembly was first demagnetized and then magnetized by an in-plane field of 2000 Oe. The external field was then removed at the point in time indicated by the arrows. The magnetization, after an initial rapid fall, remains very stable (with respect to time) even at elevated temperatures. Such stability allows us to define a meaningful critical temperature (Tc) above which Mr vanishes. As shown in Fig. 3.1(d), Tc of the 0.8MLFe/200 L Xe dot assembly is around 120 K.

This rather high Tc cannot be explained by superparamagnetic blocking if the bulk bcc Fe anisotropy (4.72 10^{5} $ergs/cm^{3}$) is assumed for the Fe dots. Using the bulk anisotropy and an average volume of $8.2nm^{3}$, the blocking temperature of the Fe dots is estimated to be no more than 2 K. Therefore, it must be the case that the ferromagnetic stability originates from either a much larger magnetic anisotropy or from dot-dot

interaction(s). To distinguish between these two factors, it is critical to be able to measure how the magnetic ordering temperature is affected when the average spacing of Fe dots is varied and the average size is fixed. A significant change of Tc would indicate that dot-dot interaction(s) play a much more dominant role than the magnetic anisotropy does, since the dot-dot interaction(s) would change with varied dot spacing, while magnetic anisotropy would not. If Tc varied little, then one would have to rule out the significance of dot-dot interactions.

We found that we could tune the average spacing and average size of the Fe dots by controlling both the Fe dosage and the Xe exposure. The effects of independently varying the Fe dosage and Xe exposure are displayed in Fig. 3.2. The density and the average size of the Fe dot assemblies are shown as a function of Fe dosage at a fixed Xe exposure of 200 L in 3.2(a), and as a function of Xe exposure at a fixed dosage of 1 ML in 3.2(b). Apparently, changing the Xe exposure has a more dramatic affect on the dot size and density than varying the Fe dosage. The fact that the dot size increases with increasing Xe exposure can be understood to result from the enhanced likelihood for Fe clusters to collide and stick to each other as they work their way toward the Cu surface through a thicker buffer layer. Based on the information in Fig. 3.2, we can find at least two sets of Fe dosage/Xe exposure The morphologies of these two Fe dot assemblies are shown in the upper images in Fig. 3.3.

The critical temperatures of the two assemblies are drastically different, despite the fact that they have the same average size. Figure 3.3 shows the remanent

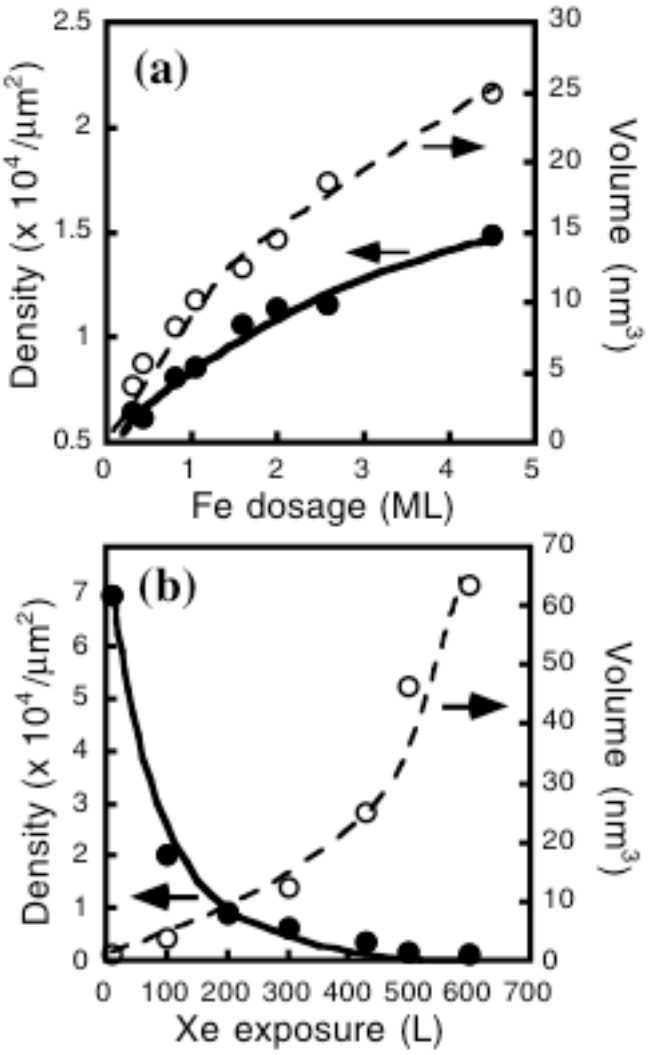

Figure 3. 2. Average size and spacing depending on Fe and Buffer Layer

Average size and density of Fe/Cu(111) dot assemblies as a function of Fe dosage (a), and Xe exposure (b). The solid and dashed lines are guides for the eyes. Two sets of Fe dosage/ Xe exposure parameter combinations can produce Fe dot assemblies with different density but the same size. They are summarized in Table I.

TABLE 3.1. Fe dot assemblies with equal size but different spacing

Fe dose (ML)	Xe exposure (L)	Average volume (nm^3)	Average density (μm^{-2})	Measured T c (K)
1.0	428	25	$3.1x10^3$	150
4.5	200	25	$1.5\ x10^4$	325
1.0	300	12	$6.2\ x10^3$	190
1.6	200	12	$1.0x10^4$	240

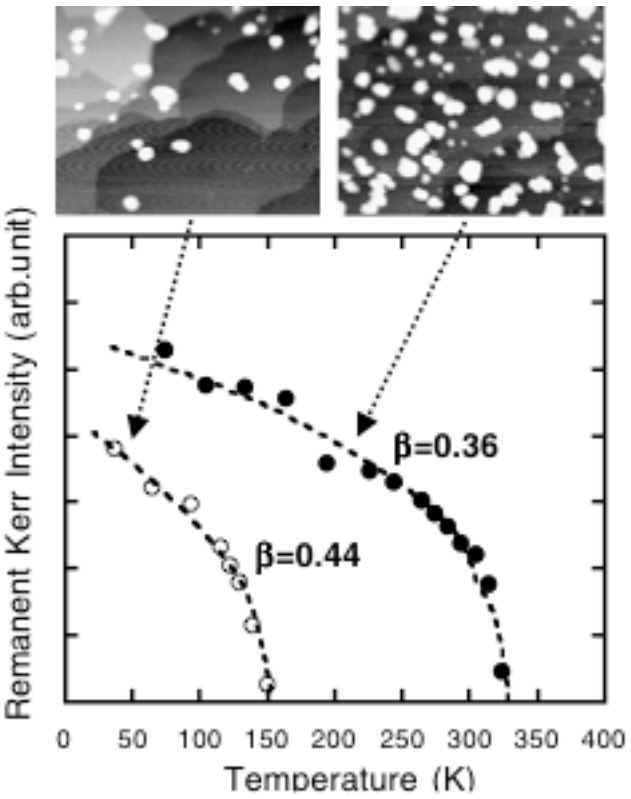

Figure 3.3. Morphology and magnetization of Fe/Cu(111) dots with equal size they are prepared by conditions highlighted in Table I.

Top: STM images (100 nm x 100 nm) of Fe/Cu(111) dots with equal average sizes (~ 25 nm 3) but different densities. Bottom: Their corresponding remanent magnetization measured as a function of temperature, with the critical exponent of power law fitting (dashed lines) indicated.

magnetization of the two dot assemblies as a function of temperature. The dot assembly (200 L Xe/4.5MLFe) with the higher density has a Tc of about 325 K, which is more than 2 times higher than the Tc of the low-density dot assembly (~ 150 K). Similar Tc enhancement is also observed in the other pair of dot assemblies as shown in Table I. Since the contribution of the magnetic anisotropy to the thermal stability of Mr in each case should be identical, the discrepancy in Tc allows us to rule out enhanced magnetic anisotropy as the root of the high-Tc ferromagnetism. This argument is also supported by a recent observation that showed the magnetic anisotropy of Co clusters approached that of bulk Co once each cluster was large enough to contain 40 atoms [17]. Considering the fact that each Fe dot in Fig. 3.3 contains about 2300 atoms in average, one would expect these Fe dots to have a magnetic anisotropy close to the bulk value.

If this is true, the magnetic anisotropy alone would only give rise to a blocking temperature of about 30 K, which is far below the observed Tc.

Having ruled out the role of magnetic anisotropy, the ferromagnetic stability of the Fe dot assemblies must originate from dot-dot interaction(s). The strength of the interaction is rather strong, as evidenced by the high Tc of the Fe dot assemblies. Based on the average dot size (8.2nm ^{3}) and density (8.05 x $10^{3}mm^{2}$) in Fig. 3.1, we can estimate the energy scale of dipolar interaction is on the order of 2.5 K. We have further performed a Monte Carlo simulation based on the actual size and position distribution from STM experiments. The simulation showed that the dipolar interaction does not lead to a Tc higher than 20 K even assuming an Ising-like anisotropy. The dipolar interaction,

however, can become significant if the spacing between the dots becomes very small, as clearly demonstrated by the work in Refs. [10,11].

Based on the aforementioned results, we conclude that a substrate-mediated, indirect exchange interaction between the Fe dots is responsible for the persistent magnetic order. To understand the exact nature of the indirect exchange interaction, it is useful to compare the Tc values of Fe dot assemblies prepared under similar conditions on various substrates. Figure 3.4 shows Tc of Fe dot assemblies prepared on Cu(111), Cu(100), and Ge(111) as a function of Xe exposure. In all cases, the Fe nominal thickness is 1 ML. Evidently, under similar growth conditions, Fe dots consistently exhibit the highest Tc on Cu(111) and the lowest Tc on semiconducting Ge(111). This again suggests that substrate-mediated interaction dominates other factors including magnetic anisotropy (including shape anisotropy) and dipolar interaction in the Fe dot assemblies. Considering the fact that Cu(111) has much more pronounced surface states than Cu(100), Fig. 4 gives a strong indication that the substrate-mediated indirect coupling is likely associated with the presence of surfaces states. More theoretical study is clearly needed to understand the role of surface states on magnetic interactions.

Because of the random spatial distribution of the Fe dots, the indirect exchange interaction should induce some degree of spin frustration in the dot assembly. The degree of the spin frustration increases with increasing density and is reflected by the ratio of the remanent to saturation magnetization (Mr/Ms). Evidence of spin frustration in this system is shown in Fig. 3.3, as the Mr of the high-density dot assembly is less than a factor of 2 higher than that of the low-density assembly, despite the fact that its Ms value is 5 times

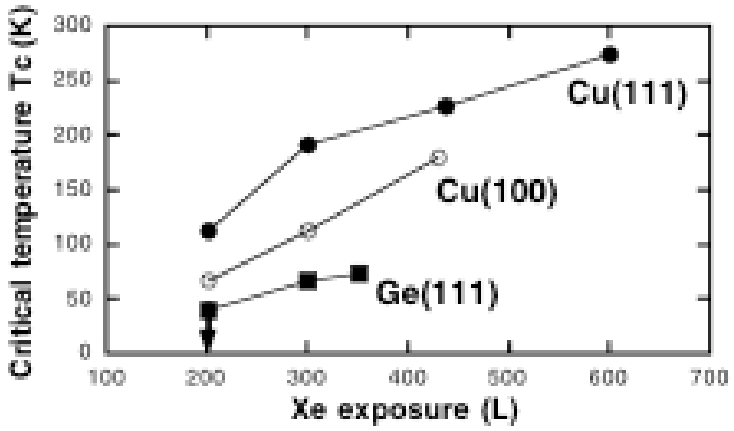

Figure 3.4. Critical temperature (Tc) of Fe dot assemblies on various substrates of Cu(111), Cu(100), and Ge(111) as a function of Xe exposure

The Fe nominal thickness is fixed at 1 ML in all cases. The arrow for the Fe=Ge111dots (200 L Xe) indicates that the Tis below 40 K.

higher. The power law fitting of the measured M vs T data that is shown in Fig. 3.3 yields distinctly different critical exponents (β) for the two assemblies. In magnetic phase transition, a decreased critical exponent is often interpreted to result from a decrease in the dimensionality of a magnetic system [18]. The change that we observe, however, may not directly link to the critical behavior of a phase transition due to the spin frustration.

In summary, we have observed an unusual ferromagnetic stability in Fe dot assemblies prepared with the aid of a Xe buffer layer on the Cu(111) surface. By growing assemblies of magnetic dots which have a fixed average size and varied spacing and then monitoring the resulting influence on the magnetic behavior, we were able to rule out enhanced anisotropy and dipolar interactions as the main contributors to the magnetic order. The strong dependence of the Tc values of Fe dots on the types of substrates suggests that the stable ferromagnetism is associated with an exchange interaction that is mediated by the substrate.

We are grateful to Zhenyu Zhang for valuable discussions. This work was supported by the Laboratory Directed Research and Development Program of Oak Ridge National Laboratory (ORNL), managed by UTBattelle, LLC for the U.S. Department of Energy under Contract No. DE-AC05-00OR22725, and by the U.S. National Science Foundation under Contract No. DMR 0105232.

Chapter 4: "Live" Surface Ferromagnetism in Fe Dot Multilayers on Cu(111)

This chapter is based on a paper already accepted in Phys. Rev. Lett. (soon to be published). The nanodot array of Fe on Cu is utilized as the base unit for a multilayer system. We observed an unusual ferromagnetic –spin glass transition, in the dimensional crossover 2D to 3D. The topmost layer remains ferromagnetic due to the strong interaction through surface state, and it is detectable because the Curie temperature is higher than the Glass temperature in the bulk. My main cntribution is the magnetic measurements.

M.A. Torija [1,2,] A.P. Li [1], C. Guan [1], E.W. Plummer [1,2], and J. Shen [1,2],*

1 Condensed Matter Sciences Division, Oak Ridge National Laboratory, Oak Ridge, TN 37831

2 Department of Physics and Astronomy, University of Tennessee, Knoxville, TN 37996

We investigate the crossover behavior from two-dimensional (2D) to threedimensional (3D) in multilayers of magnetic nanodots grown by stacking 2D Fe nanodot assemblies on Cu(111) single crystal substrate with a Cu spacing layer. Using in-situ magneto-optical Kerr effect, we have observed a striking ferromagnetic to spin-glass

phase transition with increasing number of Fe dot layers. The topmost layer of the Fe dots survives the phase transition and remains ferromagnetic. This unusual surface ferromagnetism is likely caused by a stronger surface state-mediated intralayer dot coupling which is stronger than the interlayer dot coupling, as confirmed by the fact that the critical temperature of the surface ferromagnetism is considerably higher than that of the bulk spin glass phase in the system.

Isolated noninteracting magnetic nanodots are superparamagnetic resulting from the competition between thermal fluctuation and energy barrier of magnetic anisotropy. If the spacing between magnetic nanodots is not too large, then usually the influence of magnetic interaction(s) on the superparamagnetic behavior can not be neglected. 1 It is generally recognized that there exists two types of magnetic interactions: (1) the dipole-dipole magnetostatic interaction, and (2) the electron-mediated indirect exchange interaction. The importance of the dipolar interaction is most evident in high density recording media. 2 In the strong dipolar interaction limit, Morup pointed out that a transition from a superparamagnetic state to an ordered state might occur. 3 For most nanodot systems with moderate dipolar interaction and random anisotropy, spin glass-like behavior has however been commonly observed in recent studies. [4,5,6,7,8,9,10]

The indirect exchange interaction, due to its relatively weak strength and the oscillatory nature, should have little effect on promoting a global ferromagnetic order in a randomly distributed nanodot assembly. The situation, however, can become very different at surfaces, where pronounced surface electronic states may exist to mediate a strong interaction between the magnetic nanodots. Recently, we have reported a collective

ferromagnetic behavior in two-dimensional (2D) Fe dot assemblies grown on single crystal Cu(111) surface. Experimental evidence strongly suggests that the ferromagnetic order originates from an indirect exchange interaction via the Cu(111) surface [11]. These Fe nanodots were grown using a novel method called buffer-layer assisted growth (BLAG)[12].

STM The ferromagnetic ordering temperature appears to depend strongly on the average spacing between the dots. For relatively dense nanodot assemblies, the exchange interaction is strong enough to allow the ferromagnetic order persist over room temperature. Stacking these 2D Fe nanodot assemblies with Cu spacer layer allows the formation of multilayer Fe nanodots. With increasing number of Fe dot layers, one would expect the occurrence of some sort of 2D to three-dimensional (3D) crossover. In this letter, we report that such a 2D to 3D crossover is featured by a striking ferromagnetic to spin glass transition. Remarkably, the topmost layer of the Fe dots remains ferromagnetic throughout the phase transition, creating an interesting scenario where live surface ferromagnetism prevails despite a all layers underneath become spin-glass like. The unusual surface ferromagnetism is likely caused by the fact that the surface state mediated intralayer dot coupling is stronger than the interlayer dot coupling, as confirmed by the relative critical temperatures between the surface ferromagnetism and spin glass.
The growth of the Fe multilayer dots was carried out in an ultrahigh vacuum system with base pressures better than 1 × 10-10 Torr. The Cu(111) single crystal surface was prepared by cycles of 1 keV Ne ion sputtering and annealing to 800 K, before it was cooled to about 15 K. Inert Xe gas of 5N purity was then released into the UHV chamber.

Xenon exposure was about 150 Langmuir (L). Iron of 1 monolayer equivalent was then evaporated from a wire (5N purity) that was heated by electron bombardment. The deposition rate was calibrated independently by a combination of in-situ scanning tunneling microscopy (STM), reflection high energy electron diffraction, and Auger electron spectroscopy. After Fe deposition, the sample was slowly warmed to 300 K to desorb the Xe buffer layer and allow the Fe dots to land on the Cu substrate.

A Cu capping layer of 12 ML was then deposited on the Fe dot layer at a temperature of 65 K and subsequently annealed to 300 K. The aforementioned procedure was repeated to prepare each of the additional layer of Fe dots, which gives rise to the multilayer Fe dots with controlled number of layers denoted as N. In-situ STM and magneto-optical Kerr effect (MOKE) measurements were performed layer-by-layer by briefly interrupting the growth process of the multilayer Fe dots.

The morphological appearance including the average size and the density of the Fe dots varies little from layer to layer. Fig.4.1 (a) - (c) show STM images of the multilayer Fe dots with N equals 1,4, and 10, respectively. The Fe dots have a slightly flattened hemisphere shape, with an average height of 1.2 nm, and a density of 1.2×104 / μm2. When capped by a 12 ML thick Cu layer, the Fe dots are buried completely as shown by the morphology of corresponding Cu capping layers in Fig.1 (d) - (f). Although the roughness of the Cu capping layers increases with increasing N, the exposed Cu surface consists mostly 3 layers even at N =10. This implies that most of the

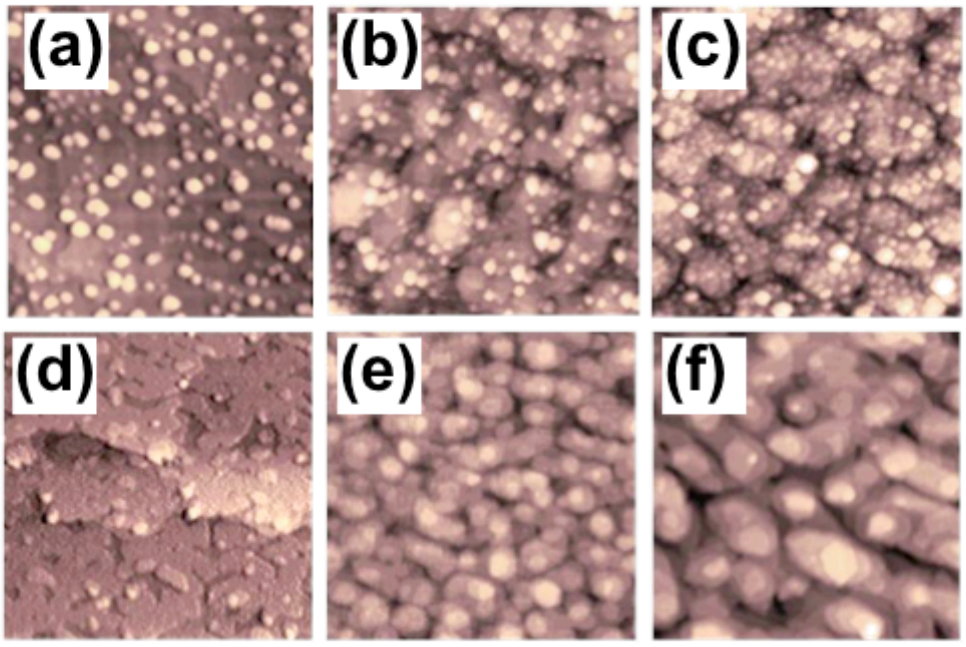

Figure 4.1. STM surface morphologies of different Fe dot multilayers.

(a), (b) and (c) are STM images acquired from N=1, 4, and 10 Fe dot layers, respectively. The exposed Fe dots are clearly visible on the surface. (d), (e) and (f) were obtained after capping 12 ML of Cu on multilayers shown in (a), (b) and (c), respectively

Fe dots in each dot layer are distributed within three atomic layers along the direction normal to the film plane. The average interlayer spacing between adjacent Fe dot layerequals to the thickness of the Cu spacer layer (~ 2.4 nm), which is considerably smaller than the intralayer spacing between the Fe dots (~ 9 nm). Knowing the size of the Fe nanodots, we estimate their superparamagnetic blocking temperature to be less than 2 K assuming that the Fe dots have the magnetic anisotropy of the bulk body-centered cubic (bcc) Fe and do no interact magnetically with each other. Magnetic measurements, however, reveal that the multilayer Fe dots have an in-plane easy magnetization axis and exhibit finite remanent magnetization (M r) at temperatures much higher than the expected blocking temperature for all N numbers. Fig.4.2 shows typical MOKE hysteresis loops measured from a Fe dot multilayer (N = 4) at various temperatures in (a), and the ratio between M r and saturation magnetization (Ms) as a function of temperatures for three multilayer Fe dots (N=1,4,10) in (b). The critical temperature (Tc), defined as the temperature at which Mr / Ms becomes zero, is about 80 K, 120 K, and 80 K for the N = 1,4,10 Fe dot multilayers, respectively.

Such non-monotonic dependence of TC on N. is most clearly demonstrated in Fig. 4.3 showing the N dependence of M s in (a) and TC in (b). Ms increases linearly with increasing N, which is expected since all the Fe dots contribute to the measured M s under the saturation field. In contrast, T C vs. N shows drastically different behavior which can be divided into three regions. As shown in Fig 4.3 (b), with increasing N, T c of the Fe dots initially increases from 80 K at N = 1 to 120 K at N = 4 (region I,). When

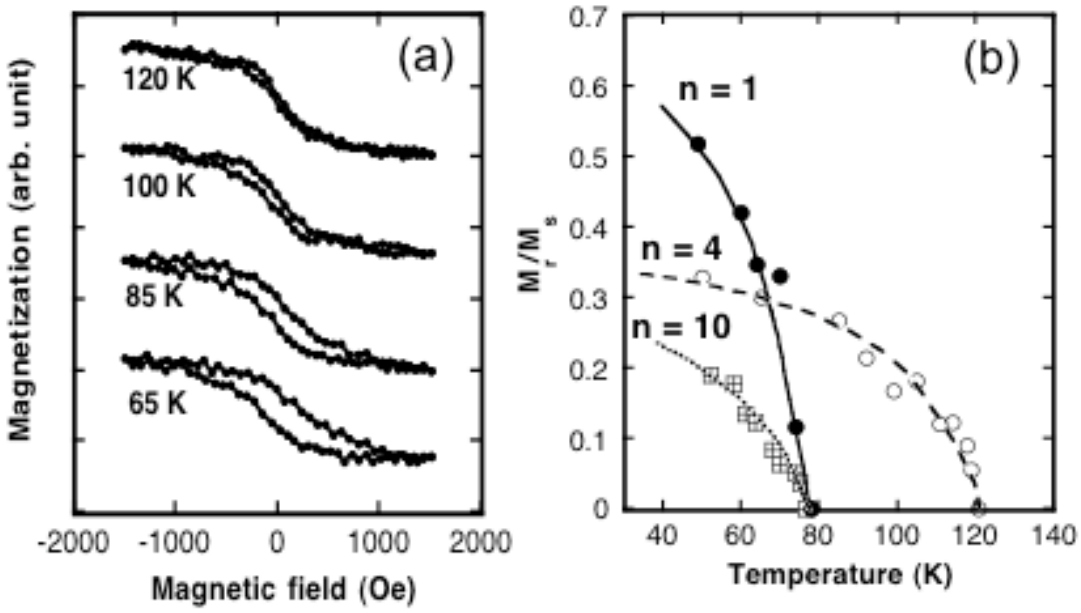

Figure 4.2 Dependence of the saturation magnetization

(a) and T c (b) on the number of Fe dot layers, N. The magnetization increases linearly with N. The Tc, however, changes nonmonotonically, and regions I, II, and III can be easily distinguished .

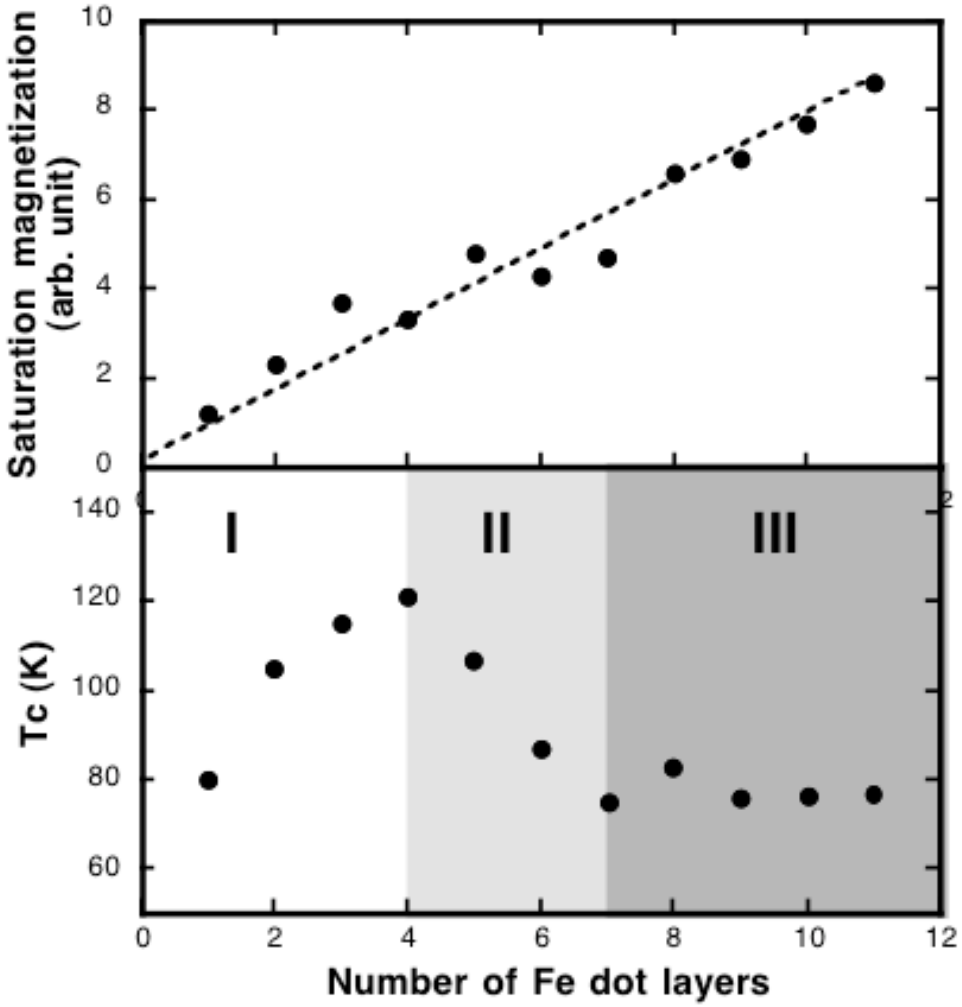

Figure 4.3 Saturation magnetization (a) and T c (b) as a function of number of Fe dot layers N. With increasing N, the M s increases linearly.

The Tc, however, changes nonmonotonically with increasing N, and regions I, II, and III are distinguished accordingly.

N is larger than 4, Tc starts to decrease, reaching the minimum temperature at N = 7 (region II). Remarkably, T c at N = 7 is almost identical to the Tc at N = 1, i.e. ~ 80 K. Further increasing N does not lead to any appreciable changes of this T c value (region III)

The fact that the multilayer Fe dots in region III ($N \geq 7$) exhibit the same Tc as the monolayer Fe dots (N = 1) is hardly a coincidence. Instead, it strongly suggests that the surface and bulk Fe dot layers have distinctly different magnetic behavior. For all thickness, the surface dot layer should be ferromagnetic owing to the surface states of Cu(111) that mediate a ferromagnetic coupling. The situation becomes totally different for Fe dots in bulk layers because the surface states no longer exist in between the Fe dots. The Fe dots underneath the surface layer still interact with each other via magnetic dipolar interaction and/or RKKY interaction. Based on previous studies of 3D random distributed interacting magnetic nanoparticles, the Fe dots underneath the surface layer likely have a spin-glass like state as the ground state. The surface ferromagnetism and bulk spin glass compete against each other resulting a changing magnetic structure with increasing thickness. At low thickness (region I), the bulk Fe dot layers can still exhibit net magnetization due to the presence of a surface ferromagnetic layer, which is why the Tc increases with increasing N in this region. In region II, the influence of the surface becomes smaller and the ferromagnetic alignment of the dot layer and hence T c starts to decrease with increasing thickness. Eventually, the system moves into region III where all Fe dot layers except the surface layer show zero Mr above the corresponding critical temperature defined as spin glass temperature (T G). The surface Fe dot layer in region

III, however, remains ferromagnetic with the same T c as that of the Fe dot monolayer because the strength of surface states mediated coupling should vary little with changing N despite the surface of the Cu capping layers in region III become somewhat rougher the Cu substrate. This can be understood by the fact that on average each Cu island is considerably larger than the Fermi wavelength of the Cu(111) surface state (~ nm) and is large enough to host many Fe dots so that the effect of roughness is minimal. The typical magnetic structures of the multilayer Fe dots in regions I, II, and III are shown schematically in Fig.4.4.

The realization of surface ferromagnetism in the Fe dot multilayers implies that the surface states mediated coupling between the Fe dots is considerably stronger than the dipolar coupling and/or bulk states mediated RKKY coupling. In another word, TG of the bulk Fe dot layers should be significantly smaller than T c of the surface dot layer. To verify this, we capped a thick Fe dot multilayer (N=11) with 20 ML of Cu and performed ex-situ superconducting quantum interference device measurements. The Cu capping should effectively "kill" the Cu surface states in the topmost Fe dot layer. The whole system should thus be in a spin glass state. Indeed, as shown in Fig. 4.5, the zero-field cooling (ZFC) and field cooling (FC) curves show strong deviation at low temperatures, which is consistent with a spin glass behavior. The corresponding T G is around 30 K and well below the T c of the surface dot layer (~ 80 K).

Finally, we note that the Fe/Cu(111) multilayer dot system closely resembles the ultrathin films of Fe/Cu(100) in their thickness dependence of Tc. In both systems,

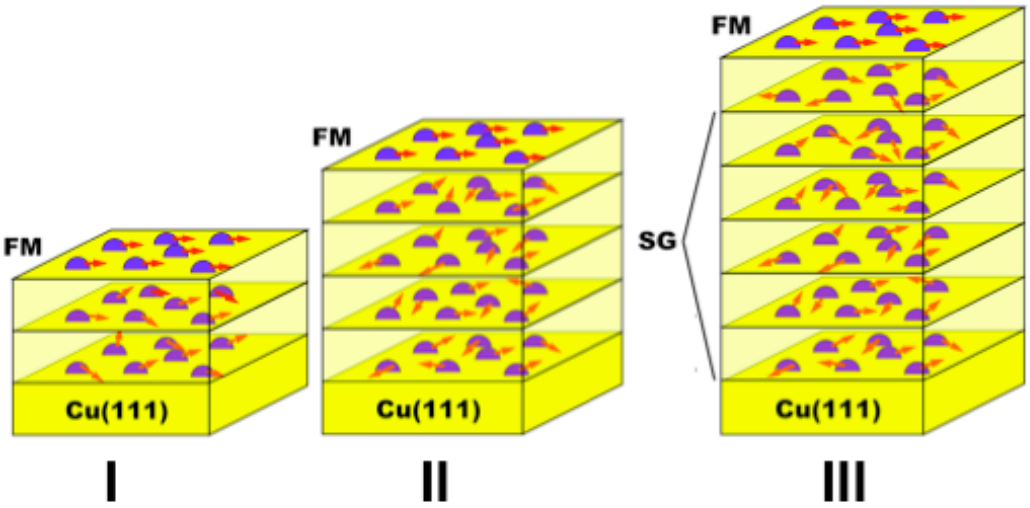

Figure 4.4. Schematic picture of the speculated spin structures of the Fe dots multilayer in regions I, II, and III.

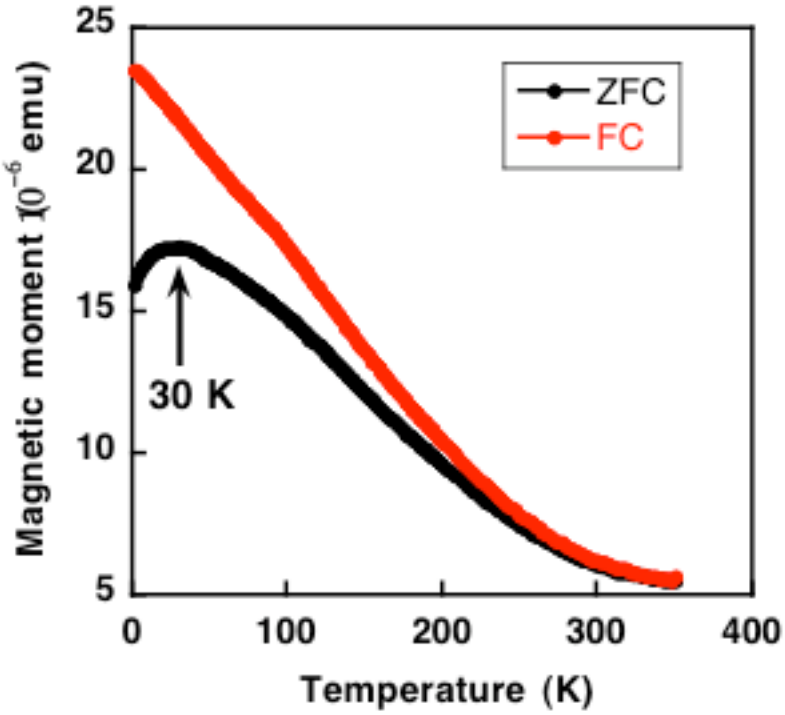

Figure 4.5. SQUID measurements in multilayer structure.

Field cooling and zero-field cooling curves of a Fe dot multilayer (N=11) measured by SQUID magnetometer.

surface ferromagnetism prevails despite all layers underneath become non-ferromagnetic at higher thickness. In the Fe/Cu(100) system, the nearest neighbor exchange interaction is so strong that the magnetic ordering and spin orientation of sub-surface layers are strongly affected by the ferromagnetic surface layer. In the artificially structured e/Cu(111) mutilayer dot system, while the surface states mediated interaction is strong enough to sustain ferromagnetism in the surface layer throughout the whole thickness regime, the interaction between the surface dot layer and the layers underneath are much weaker than nearest neighbor exchange interaction. Consequently, the dipolar and the RKKY interactions between the randomly distributed dots take over and drive the bulk layers into a spin glass like state.

This work was supported by Oak Ridge National Laboratory (ORNL), managed by UT-Battelle, LLC for the U. S. Department of Energy under Contract No. DE-AC0500OR22725, and by the U.S. National Science Foundation under Contract DMR 0105232.

Chapter 5: Frozen Low-Spin Interface in Ultrathin Fe Films on Cu(111)

This chapter examined a new morphology of Fe thin films on Cu(111). The fractal morphology yielded a magnetic transition from low to a high spin driven by thickness. A surprising feature was observed at the interface, where the bottom layer remains in the low spin phase after the phase transition. My contribution are the magnetic and morphological measurements. The articles has been published in Physiscal Review Letter vol 95, 27201 (2005)

M. A. Torija, [1,2] Z. Gai,[1,3] N. Myoung,[1,2] E. W. Plummer,[1,2] and J. Shen[1,2],

1Condensed Matter Sciences Division, Oak Ridge National Laboratory, Oak Ridge, Tennessee 37831, USA

2Department of Physics and Astronomy, University of Tennessee, Knoxville, Tennessee 37996, USA

3Department of Physics, Peking University, Beijing 100080, People's Republic of China

In ultrathin film systems, it is a major challenge to understand how a thickness-driven phase transition proceeds along the cross-sectional direction of the films. We use ultrathin Fe films on Cu(111) as a prototype system to demonstrate how to obtain such information using an in situ scanning tunneling microscope and the surface magneto-

optical Kerr effect. The magnetization depth profile of a thicknessdriven low-spin to high-spin magnetic phase transition is deduced from the experimental data, which leads us to conclude that a low-spin Fe layer at the Fe/Cu interface stays live upon the phase transition. The magnetically live low-spin phase is believed to be induced by a frozen fcc Fe layer that survives a thickness-driven fcc→bcc structural transition.

The interplay between surface and bulk often leads to thickness-driven magnetic phase transitions involving changes of magnetic order, magnetic moment, or spin orientation in ultrathin film systems [1]. Upon the phase transitions, multiple magnetic phases may coexist in thin films along both lateral and vertical directions. There is a great desire to identify these multiple phases in real space for a thorough understanding of the nature of the phase transitions. The lateral resolution is typically achieved using state-of-the-art high-resolution magnetic imaging techniques such as spin polarized scanning tunneling microscopy [2] and scanning electron microscopy with a polarization analysis [3]. The vertical distribution of magnetic phases, however, often remains unknown for most ultrathin film systems because of the lack of appropriate characterization tools.

Under special circumstances, information about magnetic phase transitions normal to surface can be obtained by indirect methods. An outstanding example is the system of ultrathin Fe films on Cu(100), in which a ferromagnetic to antiferromagnetic phase transition occurs around the 4 monolayer (ML) thickness. Above 4 ML, the coexistence of a ferromagnetic phase at the surface and an antiferromagnetic phase in layers underneath was identified by the surface magneto-optical Kerr effect (SMOKE) [4,5]. This spectacular depth profile of magnetic order represents one of the few cases in which

surface magnetism prevails, and thus has been extensively investigated ever since [6–12]. In this Letter, we report an unusual interface magnetism featuring a frozen low-spin state in a thickness-driven low spin (LS) → high spin (HS) magnetic phase transition in ultrathin Fe films on Cu(111) grown at a low temperature (LT), 65 K. Combined information from thickness dependent layer distributions and SMOKE signals indicates that a ferromagnetic LS interface layer stays live during and after the phase transition. This peculiar interface magnetism does not exist in room temperature (RT) 300 K grown Fe/Cu(111) films after a similar LS → HS phase transition. We speculate that the live LS interface in the LT Fe films originates from a frozen face centered cubic (fcc) Fe layer that survives a thickness-driven fcc →body centered cubic (bcc) structural transition.

The growth of Fe ultrathin films was carried out in an ultrahigh vacuum system with base pressures below 1 x 10 - 10 Torr. The Cu(111) single crystal surface was prepared by cycles of 1 keV Ne ion sputtering and annealing to 800 K before it was cooled to either 300 or 65 K. Iron was then evaporated from a wire (5N purity) that was heated by electron bombardment. The deposition rate was independently calibrated by a combination of in situ scanning tunneling microscopy (STM), reflection high energy electron diffraction, and Auger electron spectroscopy. After Fe deposition, in situ STM and SMOKE measurements were performed at a fixed temperature of 65 K.

Fe/Cu(111) films grown at 65 K have a perpendicular easy magnetization axis up to 3.6 ML. Figure 5.1 shows polar SMOKE hysteresis loops of the Fe films with various thicknesses. The inset shows the ratio between the remanent magnetization (Mr) and the saturation magnetization (Ms) as a function of thickness. The Mr/Ms ratio is around 20–

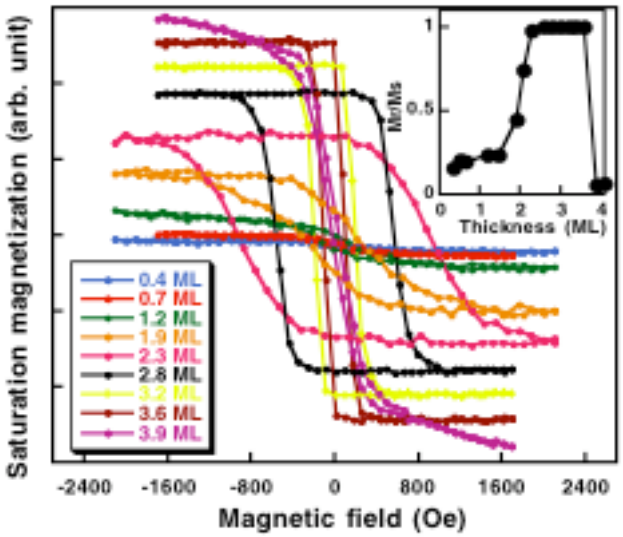

Figure 5.1 Thickness-dependent magnetic hysteresis loops of the LT-grown Fe/Cu(111) films.

It measured by polar SMOKE with the field applied perpendicular to the surface. All loops were recorded at 65 K. Inset shows the Mr/Ms ratio as a function of the thickness.

30% below 2 ML and increases to 100% at 2.2 ML. Above 3.6 ML, the Mr/Ms ratio rapidly falls to nearly zero, indicating a spin reorientation from perpendicular to in plane. Indeed, square in-plane hysteresis loops (not shown here) were detected for films above 3.6 ML. The small Mr/Ms ratio for low-thickness films is caused by the fractal island morphology as will be discussed later.

In addition to the spin reorientation, a LS →HS phase transition has also been observed in the LT Fe/Cu(111) films. Figure 5.2 shows Ms (in arbitrary units) deduced from SMOKE for both RT and LT-grown Fe films as a function of the thickness. For both types of films, Ms increases linearly with a slope that changes from a same small value at lower thickness to a same large value at higher thickness. The critical thickness for the slope change is around 2 and 1 ML for the RT and LT films, respectively. Based on previous studies, the slope change for the RT Fe/Cu(111) films reflects a LS → HS magnetic phase transition that is associated with a fcc → bcc structural transition [13–15].

The transformed HS phase has a magnetic moment of 2.2 μB, which corresponds to that of the bcc Fe. Considering that the LT Fe films show a similar slope change, one may conclude that a similar LS → HS phase transition occurs in the LT Fe/Cu(111)films, though at a lower thickness of 1 ML.

However, there exists a striking difference between the LS→HS transitions in the LT and the RT films. For the RT films, after transition, Ms linearly increases with the thickness on a line that extrapolates back to zero point, which reflects a uniformly

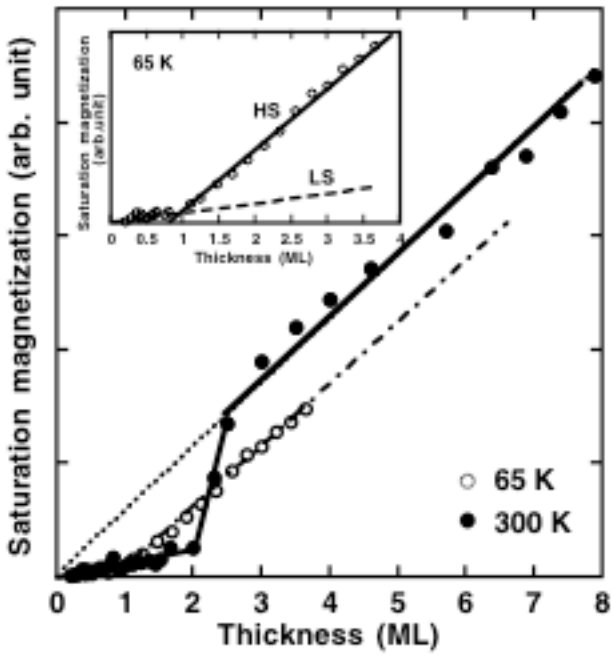

Figure 5.2 Kerr signals measured at 65 K for both LT and RT grown Fe/Cu(111) films as a function of thickness

The inset shows the extrapolation from the high slope of the Kerr signals of the LT-grown films becomes zero at 0.8 ML thickness

magnetized HS phase. This is obviously not the case in the LT Fe films. As shown in the inset of Fig. 2, the extrapolation of Ms of the transformed LT Fe films reaches zero already at 0.8 ML. While this often implies the existence of a magnetically dead layer, the fact that the films are in a ferromagnetic LS phase before the transition indicates that the situation should be more complicated in the LT Fe/Cu(111) system.

To fully understand this rather unusual LS → HS transition in the LT films, it is critical to obtain information on the layer-resolved magnetic moment throughout the transition. To do this, one first has to know the layer distribution of the films during growth. Figure 5.3 shows the STM images of LT-grown Fe films that were acquired in situ at the growth temperature of 65 K. Because of the diffusion limited aggregation at low temperature [16], all islands have a fractal shape at a submonolayer thickness. The fractal islands are virtually formed by nanometer-sized clusters instead of single atoms. The fractal morphology for LT Fe films differs dramatically from the morphology of RT grown Fe films, which are characterized by quasitriangular shaped islands as shown in the inset of the 1.05 ML image. With increasing thickness, the fractal islands grow larger and percolate morphologically when the nominal thickness reaches ~1.5ML. This explains why the Mr/Ms ratio only starts to increase quickly beyond 1.5 ML in Fig. 1, since before percolation the isolated fractal islands should have a low superparamagnetic blocking temperature so that they do not contribute to remanent magnetization. Further increasing the thickness leads to a surface roughening process. A detailed data analysis reveals that the roughness follows a power-law dependence on film thickness with a

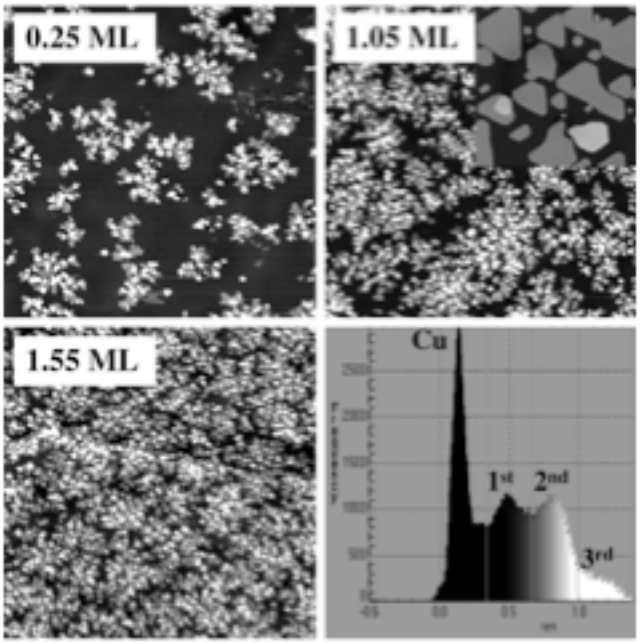

Figure 5.3. STM images of LT-grown Fe/Cu(111) films.

The inset in the 1.05 ML image is the morphology of a RT grown Fe/Cu(111) film with the same thickness and the same scanning area. The histogram of the LT- grown 1.05 ML image is shown in the lower right. The labels of Cu, 1st, 2nd, and 3rd correspond to the terraces of bare Cu, and the 1st, 2nd, and 3rd layer of Fe, respectively.

growth exponent of 0.36, which is reasonable for diffusion limited growth at low temperatures [17,18].

The layer fillings can be obtained as a function of the film thickness by analyzing the height histogram of the STM images. A typical histogram calculated from the 1.05 ML film image is shown in the lower right in Fig. 5.3. Once the histogram peaks are identified, the coverage for each layer can be calculated straightforwardly. Repeating this procedure for each thickness, we obtained the layer filling curves in the upper panel of Fig. 4. Combining the information from the thickness-dependent saturation magnetization (Fig. 2) and the layer filling (Fig. 4), we are able to obtain the depth profile of the magnetization of the films upon the LS → HS magnetic phase transition. This is done by assuming that the Fe films do not have any antiferromagnetic alignment between different layers, which is reasonable due to the linear increase of Ms in the LS phase. In any case, layer-wised antiferromagnetism has not yet been observed in the (111)-oriented fcc Fe films and is thus not considered here. The fitting procedure is then carried out with the following restrictions: (1) the magnetization density takes values of 0 μ_B, 2.2 μ_B, or any other values in between (for the LS phase); (2) the HS phase has a fixed 2.2 μ_B moment. Although the SMOKE data do not give the absolute values of magnetization, the layer-resolved magnetization can still be quantified by assuming that the larger increasing slope in Fig. 5.2 represents a value of 2.2 μ_B. Figure 5.4 (lower panel) shows the best fitting curve for the thickness-dependent saturation magnetization, along with the schematic depth profile of the magnetization that yields the best fitting. Remarkably, upon the LS →HS phase transition, the films are magnetically nonuniform in both lateral

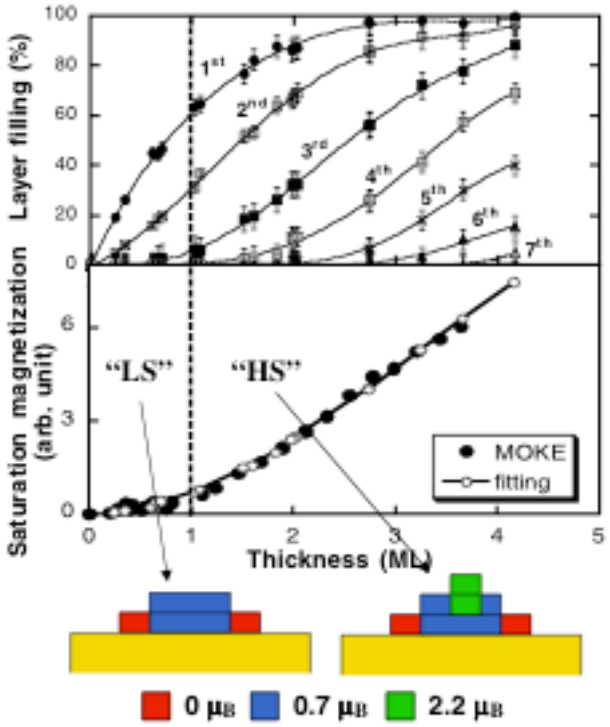

Figure 5.4. Layer distributions (upper panel) of the LTgrown Fe/Cu(111) films.

Based on the layer distribution, the best fit of the measured SMOKE data is obtained based on the model shown in the lower panel.

and vertical directions. At the initial stage of growth, the topmost surface of the film consists of both 1st and 2nd layers of Fe. All Fe atoms that are in the exposed 1st layer have zero net moment, while all Fe atoms in the bilayer regions have a moment of 0.7 μ_B. With increasing thickness, 3rd layer islands start to appear. All Fe atoms in the 3rd layer and its shadowed 2nd layer regions become HS polarized with a net moment of 2.2 μ_B, though the 1st layer Fe atoms stay LS polarized (0.7 μ_B). Further added Fe atoms on top all have a moment of 2.2 μ_B without changing the LS state of the 1st layer Fe.

This rather complicated LS→HS phase transition is likely associated with an equally complicated fcc to bcc structural transition, which was observed to occur between 1 and 2 ML for LT-grown Fe/Cu(111) films [19]. It has been well known that fcc Fe can have multiple magnetic phases ranging from nonmagnetic to HS ferromagnetic depending on the actual lattice constant [20]. The bcc Fe, on the other hand, has a rather robust moment of 2.2 μ_B. Based on our fitting data in Fig. 5.4, we conclude that the first two layers of Fe have a distorted fcc-like structure, which is in a LS phase. The addition of a 3rd layer of Fe atoms leads to a local structural transition from fcc to bcc in its shadowed regions except the 1st layer. The 1st layer, due to a strong interaction with the fcc Cu substrate and the low temperature, freezes into the fcc structure and thus the LS state. To verify whether it is the low substrate temperature that freezes the LS state at the Fe/Cu interface, we have performed similar SMOKE measurements on Fe/Cu(111) films grown at 90 and 175 K. Indeed, while the 90 K films behave similarly to the films grown at 65 K, the 175 K films are uniformly magnetized in a HS state after the fcc to bcc structural transition. These experiments indicate that the LS interface results from the low substrate

temperatures due to the suppressed thermal diffusion. In conclusion, we have observed an unusual LS→HS phase transition in ultrathin Fe films on Cu(111) grown at 65 K. Upon phase transition, the layer-wise distribution of the magnetic moment becomes highly nonuniform associated with a complicated fcc to bcc structural transition. The Fe layer at the Fe/u interface freezes into a LS state despite all layers above becoming HS polarized.

This work was supported by Oak Ridge National Laboratory (ORNL), managed by UT-Battelle, LLC for the U.S. Department of Energy under Contract No. DEAC05-00OR22725, and by the U.S. National Science Foundation under Contract No. DMR 0105232

Chapter 6: Summary

The intriguing properties observed at the nano scale and potential applications to computational devices place the study of nano-magnetism at the forefront of the nano-technology revolution. Recent advances in materials synthesis and nanofabrication have made it possible to create a wide range of nanomagnetic systems with unprecedented precision. This in turn has created opportunities to further explore novel magnetic phenomena. This thesis explored some new and interesting phenomena in nanomagnetism, resulting in a number of relevant contributions to this field of study. This final chapter summarizes the important discoveries, highlights new avenues in fundamental research, and discusses research topics meriting future study.

We first examined an interesting magnetic interaction that stabilized Magnetization in the Fe on a Cu(111) substrate system. The role of the substrate was already known to be the principle factor altering growth kinetics and anisotropy. However, it was observed that Fe nanodots on a Cu(111) substrate also contributed directly to the coupling of the magnetization. We discovered that the electronic structure (polarization of surface states) of the substrate influences the magnetic interactions within the nanostructure.

This interesting ferromagnetic behavior is driven by the phenomena discussed in the chapter 4. The pilling of these arrays created a peculiar system where the bulk ground

state was a spin glass, but the surface ferromagnetism (from the top uncapped layer) was still observable.

Researchers have predicted that some systems will manifest differential magnetism in bulk versus that of the surface. Differing atomic coordination number and/or surface reconstruction is attributed to be the causal mechanism (by distortion of the unit cell). An example is a thin film of Fe on Cu (100). However, the origin of the differential magnetic states in this system is the weight of the different magnetic interactions in the bulk versus that of the surface. In the Fe nanodot system, the indirect exchange through the surface is strong enough to drive the ferromagnetism.

In the bulk, when this interaction disappears, the dipolar and RKKY interaction combined with random anisotropy, drives the system to a spin glass. Moreover, engineering a system that can differentiate the surface and the bulk magnetism is a remarkable achievement.

Magnetic properties of Fe on Cu are very complex, and they depend on a large number of parameters. One of the reasons is the instability of the magnetism as the unit cell volume changes. Different substrates, morphologies and capping layers directly affect the volume, and subsequently yield differing magnetic order. This volume instability is a precursor of the phase transitions driven by thickness.

Chapter 5 discussed an excellent example of magnetic phase transformation. Fractal morphology transforms to a different phase which leaves the interface intact. This phenomena has never been observed in any Fe on Cu(111) system. The critical

temperature and critical thickness for spin reorientation can be tuned by manipulating the system morphology.

In the appendix 2, reduced dimensionality of FeGe nanowires displayed interesting properties. A particularly interesting observation was that this material is antiferromagnetic in bulk, but becomes ferromagnetic when grown in nanostructure form. We have shown how epitaxial strain due to a slight mismatch with the Ge(111) substrate is responsible for stabilizing the unusual ferromagnetic ordering. The changes in the unit cell are responsible for a different ground state based on the same volume instability. Therefore, we have shown again how in the nanoscale the stability of materials out of equilibrium is possible. This challenges our understanding of these systems and offers the opportunity of crafting materials with a new suite of physical behaviors.

6.1 Open questions

We have demonstrated that the electronic structure of the substrate can drastically influence magnetic interactions. But its origin is still elusive and has been mainly studied by indirect observations: modifications of the surface or the study of competition with other phenomena. Better, more direct techniques are needed to improve our understanding of the role of substrate states. The use of high resolution Spin Dependent STM might lead to more useful, better quality data. Unfortunately, definitive answers have not been provided thus far.

Another method involves the application of Photoemission spectroscopy to buried surfaces. Recent studies in Mg (1000) on W have proven the viability of this technique, but even when the experimental results are in agreement, the interpretation has been, in most cases, a source of conflict [1,2]. As for further indirect measurements, it is possible to study the same nanodot Fe assemblies on top of twinned surfaces, such as Au (111) or Ag (111), and compare them with Au (100) and Ag (100). The (111) surfaces of Ag and Au have already been shown to exhibit surface states by photoemission [3]. The nexus between (111) surfaces in novel metals and magnetism has been addressed in Kondo Phenomena, [4-5]. These kinds of studies can give an indication of which feature, difference in energy, density of states, or position with respect to the energy of the bands, will be more relevant.

Nanotechnology in general, and spintronics in particular, are driven by the search for small magnets with stable remanence magnetization at room temperature, that also possess a low coercitivity field. When studying the competition of strong ferromagnetism and spin glass behavior in Fe/Cu multilayered systems, we noted that dipolar interactions and random anisotropy were the common factors. We then asked the question of whether it is possible to control these factors in a random distribution so the frustration decreases. In this sense, superparamegnetic nanoparticles constitute a new avenue to discover and observe new phenomena. As stated, the control and stabilization of magnetism in nanodots has potential usage for high capacity computational storage

devices. This is an important reasons why both industry and scientists are interested in nano-magnetic research.

Another fundamental question is whether the frozen interface disappear with temperature. More compact devices could be manufactured if different magnetic properties could be 'designed' using the same system. The challenge lies in growing stable structures at room temperature or lower. It will require overcoming the difficult task of creating controlled, non-random distributions via self-assembly methods. The physics and engineering challenges are complex and will require extensive research and creativity to understand and manipulate the observed phenomena.

These challenges will be overcome, and ferromagnetic semiconductors will be used in future generations of integrated circuits. and will be combined in spin injection devices. This will require transport studies that obviously cannot be carried out on a Ge substrate. The possibility of 'self supported' FeGe wires with the same magnetic properties would require new techniques that are probably beyond the capabilities of current Ultra High Vacuum techniques.

In closing, it must be stated that our approach is not constrained to the studied systems. New degrees of complexity and unexpected phenomena may appear in novel, intrinsically more complex nano-materials as well, (TMO or piezo-electric) where electronic, lattice and spin degrees of freedom are interconnected.

REFERENCES

Chapter 1.

1.1http://www.tcd.ie/Physics/Schools/what/materials/magnetism/top.html.

1.2.http://www.tcd.ie/Physics/Schools/what/materials/magnetism/two.html

1.3http://www-istp.gsfc.nasa.gov/Education/whmfield.html

1.4Ferromagnetism and Electronic Correlations W. Nolting Humboldt-Universitat zu Berlin, Institut fur Physik, Lehrstuhl Festkorpertheorie, InvalidenstraBe 110 10 115 Berlin, Germany

1.5 *Spin-wave modes in magnetic nanowires,* R. Skomski, M. Chipara, and D. J. Sellmyer ,J. Appl. Phys. 93, 7604 (2003)

1.6*Giant Magnetoresistance of (001)Fe/(001)Cr magnetic superlattices,* M.N. Baibich, J.M. Broto, A. Fert, F. Nguyen van Dau, and F. Petroff, Phys. Rev. Lett. 61, 2472 (1998).

Magnetic Coupling in the Co/Cu/Co(100) System with Momentum- Resolved Quantum Well State, R. K. Kawakami, E. Rotenberg, Ernesto J. Escorcia-Aparicio, Hyuk J. Choi, J. H. Wolfe, N. V. Smith, and Z. Q. Qiu , *'Determination of the*, , Phys. Rev. Lett, 82 , 4098 (1999)

1.6 '*Tailoring magnetism in artificially structured materials: the new frontier'* J.Shen and J.Kirschner, Surf. Sci. 500, 300 (2002)Frontiers in Surface Science

1.7 *Absence of Ferromagnetism or Antiferromagnetism in One- or Two-Dimensional Isotropic Heisenberg Models,* N. D. Mermin and H. Wagner, Phys. Rev. Lett. 17, 1133-1136 (1966)

1.8 *Ferromagnetism of ultrathin films* M. Bander and D. L. Mills, Phys. Rev. B 38,

12015-12018 (1988)

1.9 *Submonolayer Magnetism of Fe(110) on W(110): Finite Width Scaling of Stripes and Percolation between Islands* H. J. Elmers, J. Hauschild, H. Höche, U. Gradmann, H. Bethge, D. Heuer, and U. Köhler Phys. Rev. Lett. 73, 898-901 (1994)

1.10 *Structural and magnetic phase transitions of Fe on stepped Cu(111)* J. Shen, M. Klaua, P. Ohresser, H. Jenniches, J. Barthel, Ch. V. Mohan, and J. Kirschner Phys. Rev. B 56, 11134-11143 (1997)

1.11 *The remarkable difference between surface and step atoms in the magnetic anisotropy of two-dimensional nanostructures* S. Rusponi T. Cren, N. Weiss, M. Epple, P. Buluschek, L. Claude and H. Brune *Nature Materials* 2, 546–551 (2003)

1.12 *A Mechanism if Magnetic Hysteresis in heterogeneous alloys*, E.C. Stoner and E.P. Wohlfarth Philos. Trans. R. Soc. London A 240 (1948) 599

1.13. L. Neel, Ann Geophys, 5 (1949) 99

1.14 *Thermal fluctuation of a single domain particle* W.F. Brown,, Phys. Rev. 130 (1963)

1.15 *Theoretical relaxation –times of large superparamagnetic particles with cubic anisotropy, A. Aharoni and I. Einstein*, Phys. Rev. B 11 (1975) 514

1.*16 Magnetic method for the mesumerent of precipitate particle sizes in a Cu-Co alloy*, J.J. Becker, Trans. Am. Inst. Mining. Met. Petrol. Engrs. 209, 59 (1957)

The anisotropy of very small Co particles, C.P. Bean,J.D. Livingstton and D.S. Rodbell, J. Phys. Etla Radium 20 (1959)298.

1.17 *Saturation of Magnetization and Size of Iron Particles less than 100A in diameter,* F.E.Luborsky and P.E. Lawrence, J. Appl. Phys. 32, Suppl.(1961) 231S

1.18 *Magnetism form the atom to the bulkin iron cobalt and nickler clusters*, J.P. Bucher, D.C. Chatelain and W.A. de Heer, Science 265 (1994) 1682

1.19 *Magnetic properties of free cobalt clusters*, J.P. Bucher, D.C. Douglas, and LA. Bloomfield, Phys.Rev.Lett. 66(1991 3052

1.20 *Suface-enhanced magnetism in nickel clusters*, S.E. Apsel, J.W. Emmert, J.Deng, and L.A. Bloomfield, Phys. Rev. Lett. 76 (1996) 1441

1.21 *Experimental observation of magnetism in rhodium clusters*, A.J. Cox, J.G.Louderback, and L.A. Bloomfield, Phys. Rev. Lett. 71 (1993) 923

1.22 C.P. Bean and J.D. Livigstton, J.Appl. Phys. 30 suppl. (1959)1202

1.23 *Magnetism of nanometer scale iron particles arrays*, S. Wirth, S. von Molnar, M.Field and D.D. Awschalom, J. Appl. Phys. 85 (1999) 5249

1.24 *Single-domain circulas nanomagnetis*, R.P. Cowburn, D.K. Koltsov,A.O. Adeyeye, M.E. Welland, and D.M. Tricker,

1.25, *Superparamagnetic relaxation of weekly interacting particles*, S. Morup and E. Tronc, Phys.Rev. Lett. 72 (1994) 3278

1.26 *Influence of the dipoalar interaction on magnetic properties of the ultrafine ferromagnetic particles*, Phys. Rev. Lett. 84 (2000) 167

1.27 *Probing antiferromagnetic coupling between nanomagnets* R. P. Cowburn
Phys. Rev. B 65, 092409 (2002)

1.28 *Micromagnetics of ferromagnetic equilateral triangular prisms* D. K. Koltsov, R. P. Cowburn, and M. E. Welland J. Appl. Phys. 88, 5315 (2000)

1.29 *Room Temperature Magnetic Quantum Cellular Automata* R. P. Cowburn and M. E.

Welland *Science* (2000) 287

1.30 *Magnetoresistance behaviour of magnetostatically coupled Ni80Fe20 wires*

A. O. Adeyeye, R. P. Cowburn and M. E. Welland Journal of Magnetism and Magnetic Materials, Volume 213, Issues 1-2, (2000), Pages 1-*6*

1.31 *Layered Magnetic Structures: Evidence for Antiferromagnetic Coupling of Fe Layers across Cr Interlayers* P. Grünberg, R. Schreiber, and Y. Pang*

M. B. Brodsky and H. Sowers Phys. Rev. Lett. 57, 2442–2445 (1986)

1.32 *Antiparallel coupling between Fe layers separated by a Cr interlayer: Dependence of the magnetization on the film thickness* C. Carbone and S. F. Alvarado Phys. Rev. B 36, 2433 (1987

1.33 *Observation of a Magnetic Antiphase Domain Structure with Long-Range Order in a Synthetic Gd-Y Superlattice* C. F. Majkrzak, J. W. Cable, J. Kwo, M. Hong, D. B. McWhan, Y. Yafet, and J. V. Waszczak, C. Vettier Phys. Rev. Lett. 56, 2700 (1986)

1.34 *Long-range incommensurate magnetic order in a Dy-Y multilayer*

M. B. Salamon, Shantanu Sinha, J. J. Rhyne, J. E. Cunningham, Ross W. Erwin, Julie Borchers, and C. P. Flynn Phys. Rev. Lett. 56, 259 (1986)

1.34 *Systematic variation of the strength and oscillation period of indirect magnetic exchange coupling through the 3d, 4d, and 5d transition metals* S. S. P. Parkin. Phys. Rev. Lett 67 3598 (1991)

1.35 *Indirect Exchange Coupling of Nuclear Magnetic Moments by Conduction Electrons*

M. A. Ruderman and C. Kittel Phys. Rev. 96, 99–102 (1954)

1.36 *Spin polarization in p-bands of copper in cobalt/copper multilayers* J. -F. Bobo, M. Piecuch, S. Pizzini, A. Fontaine, E. Dartyge, Ch. Giorgetti and F. Baudelet, J. Magn Magn. Mater. 126, 251 (1993)

1.37 *Period of oscillatory exchange interactions in Co/Cu and Fe/Cu multilayer systems* R. Coehoorn, Phys. Rev. B 44 9331 (1991)

1.38 *Oscillatory coupling between ferromagnetic layers separated by a nonmagnetic metal spacer* P. Bruno and C. Chappert, Phys. Rev. Lett. 67 1602 (1991)

1.39 *Ruderman-Kittel theory of oscillatory interlayer exchange coupling* P. Bruno and C. Chappert, Phys. Rev. B, 46 261 (1992)

1.40 *Electronic Stability of Magnetic Fe/Co Superlattices with Monatomic Layer Alternation* G. A. Farnan, C. L. Fu, Z. Gai, M. Krcmar, A. P. Baddorf, Zhenyu Zhang, and J. Shen Phys. Rev. Lett. 91, 226106 (2003)

1.41 *Nearly total spin polarization in La2/3Sr1/3MnO3 from tunneling experiments* M. Bowen, M. Bibes, A. Barthélémy, J.-P. Contour, A. Anane, Y. Lemaître, and A. Fert Appl. Phys. Lett. 82, 233 (2003)

1.42 *Tunneling of electrons in conventional and half-metallic systems: Towards very large magnetoresistance* A. M. Bratkovsky, Phys. Rev. B 56 2344 (1997)

1.43 *Current-induced domain-wall switching in a ferromagnetic semiconductor structure* M. Yamanouchi, D. Chiba, F. Matsukura, and H. Ohno Nature 428, 539 (2004)

1.44. *Spin Transport and Localization in a Magnetic Two-Dimensional Electron Gas*, I. P. Smorchkova and N. Samarth, J. M. Kikkawa and D. D. Awschalom Phys. Rev. B 58,

R4238 (1998)

Chapter 2

2.1Revisions of basic concept in magnetism can be found in:

Introduction to Magnetism and Magnetic Materials, Jiles, (Chapman and Hall)

Introduction Solid State State, Myers (Taylor and Francis)

Magnetism in Low dimensionality, S.D. Bader Surf. Sci. 500 172-188 (2002)

Introduction to Solid State Physics, Kittel, (Wyley and Son) (1997)

Permanent Magnetism, Skomski and Coey, IoP, (1999)

2.2.'Theorie du Trainage Magnetique des Ferromagneticques en Grains, Avec Applications Aux Terres Cuites' L. Neel Ann Geophys 599 (1949)

2.3 'Superparamagnetism and Spin Glass Ordering in Magnetic Nanocomposites', S.Morup Euraphys. Lett. 28 671 (1994).

2.4 'Oscillatory exchange coupling in Fe/Cr multilayers', M. D. Stiles Phys. Rev. B. 54 14679 (1996)

Tailoring magnetism in artificially structured materials: the new frontier' J.Shen and J.Kirschner Surf. Sci. 500, 300 (2002)

2.5 'Repusive Casimir Forces', Kenneth et al Phys. Rev. Lett, 89, 033001, (2002)

2.6, Shell Effect in Exchange Coupling of Transition Metal Dots and Their Arrays," V.N. Kondratyev and H.O. Lutz Phys. Rev. Lett. 81, 4508 (1998)

,Absence of ferromagnetism or antiferromagnetism in one – or two- dimensional isotropic Heisemberg models', N.D.Mermin and H.Wagner Phys. Rev. Lett. 17, 1133 (1966)

2.7 'Thermoinduced Magnetization in Nanoparticles of Antiferromagnetic Materials', S. Morup and K. Frandsen Phys. Rev. Lett. 92, 217201 (2004).

2.8 'Surface MagnetoOptic Kerr effect (SMOKE)', Z.Q. Qiu and S.D. Bader, J. MAgn. Magn. Mater. 200, 664 (1999)

2.9'Scanning Tunneling Microscopy', G. Binning and H. Rohrer, Helv. Phys. Acta 55, 726 (1982)

Chapter 3

3.1 '*Spontaneous magnetic order in random dipolar solids'*, H. Zhang and M. Widom, Phys. Rev. B 51, 8951 (1995).

3.2 *'Monte Carlo studies of the dynamics of an interacting monodispersive magnetic-particle system'*J.-O Andersson, C.Djuberg,T. Jonhsson, P. Svedlindh and P. Nordblad et al., Phys. Rev. B 56, 13 983 (1997).

3.3 '*Magnetic Properties of Dipolar Interacting Single-Domain Particles'*D. Kechrakos and K. N. Trohidou, Phys. Rev. B 58,12169 (1998).

3.4 T. Jonsson, P. Nordblad, and P. Svedlindh, Phys. Rev. B 57, 497 (1998).

3.5 .'*Calculations of the susceptibility if interacting superparamagnetic particles'*R. W. Chantrell et al., Phys. Rev. B 63, 24 410 (2000). [

3.6 '*Colective Magnetic properties of cobalt nanocrystals self assembled in a hexagonal network: Theoretical model supported by experiments'*. V. Russier C. Petit, J. Lengrand, and M.P. Pileni,., Phys. Rev. B 62, 3910 (2000).

3.7 '*Reorinetational magnetic transition in high-density arrays of single-domain dots'*K. Yu. Guslienko, S. Choe, and S. Shin, Appl. Phys. Lett. 76, 3609 (2000).

3.8 *'Dipolar Interaction between two-dimensional magnetic particles*'P. Politi and M. G. Pini, Phys. Rev. B 66, 214414 (2002).

3.9 '*Effect of interdot magnetostatic interaction on magnetization reversal in circular dot arrays'* V. Navosad, K. Yu Guliesko, H. Shima, Y. Otani, S. G. Kim, K. Fukamichi, N. Kikuchi, O. Kitakami, and Y Shimada., Phys. Rev. B 65, 60402 (2002).

3.10 U. Bovensiepen et al., J. Magn. Magn. Mater. 192, L386 (1999).

3.11 P. Poulopoulos et al., Phys. Rev. B 65, 064431 (2002).

3.12 '*Magnetic Moment of fcc Fe(111) Ultrathin Films by Ultrafast Deposition on Cu(111)*', J. Shen, P. Ohresser, Ch. V. Mohan, M. Klaua, J. Barthel, and J. KirschnerPhys.Rev. Lett. 80 1980 (1998)

3.13 '*Magnetism in one dimension: Fe on Cu(111)*,', Phys. Rev. B. 56, 2340] J. Shen et al., Phys. Rev. B 56, 2340 (1997).

3.14 '*Structural and magnetic phase transitions of Fe on stepped Cu(111)*'J. Shen, R. Skomski, M. Klaua, H. Jenniches, S. Sundar Manoharan, and J. Kirschner, , Phys. Rev. B. 56 11134 (1997).

3.15 *'Buffer-Layer-Assisted Growth of Nanocrystals: Ag-Xe-Si(111)'*Huang, S. J. Chey, and J. Weaver, , Phys.Rev. Lett. 80, 4095 (1994)

3.16 STM line profiles often exaggerate the lateral size of the dots due to tip effect. The lateral size of the dots was thus calculated based on the nominal thickness, dot density, and dot height.

3.17 '*Giant Magnetic Anisotropy of Single Cobalt Atoms and Nanoparticles'*,P. Gambardella, S. Rusponi, M. Veronese, S. S. Dhesi, C. Crazioli, A. Dallmeyer, I. Cabria, R. Zeller, P. H. Dederichs, K. Kern, C. Carbone, and H. Brune, Science 300, 1130 (2003)

3.18 *'Buffer-Layer-Assisted Growth of Nanocrystals: Ag-Xe-Si(111)'*F. Huang et al., Phys. Rev. B 49, 3962 (1994).

Chapter 4

4.1 "*Models of the Dynamics of Interacting magnetic Particles"* M.F. Hansen and S. Morup, J. Magn. Magn. Mater. 184,262 (1998).

4.2 **"***Nanostructured magnetic films for extremely high density recording"* D.J. Sellmyer, M. Yu, and R.D. Kirby, Nanostruct. Mater. 12, 1021 (1999).

4.3 '*Superparamagnetism and Spin Glass Ordering in Magnetic Nanocomposites'*S. Morup, Europhys. Lett. 28, 671 (1994).

4 4'*Aging in a magnetic particle system'* T. Jonsson, J. Mattsson, C. Djurberg, F. A. Khan, P. Nordblad, and P. Svedlindh, Phys. Rev. Lett. 75, 4138 (1995).

4.5 C.,' *Dynamics of an Interacting Particle System: Evidence of Critical Slowing Down'* Djurberg, P. Svedlindh, and P. Nordblad,M. F. Hansen, F. Bødker, S. Mørup , Phys. Rev. Lett. 79, 5154 (1997).

4.6 , '*Static Scaling on an Interacting Magnetic Nanoparticle System'* T. Jonsson, P. Svedlindh, and M.F. Hansen, Phys. Rev. Lett. 81, 3976 (1998).

4.7 '*Blocking and Freezing of Magnetic Moments for Iron Nitride Fine Particle Systems'*H. Mamiya, I. Nakatani, and T. Furubayashi, Phys. Rev. Lett. 80, 177 (1998).

4.8 *'Slow Dynamics for Spin-Glass-Like Phase of a Ferromagnetic Fine Particle System'*H. Mamiya, I. Nakatani, and T. Furubayashi, Phys. Rev. Lett. 82, 4332 (1999).

4.9 *'Nonequilibrium dynamics in an interacting Fe-C nanoparticle system'*P. Jonsson, M.F. Hansen, P. Nordblad, Phys. Rev. B 61, 1261 (2000).

4.10 '*Memory effect in an Interacting Magnetic Nanoparticle System'*Y. Sun, M.B. Salamon, K. Garnier, and R.S. Averback, Phys. Rev. Lett. 91, 167206 (2003).

4.11 *Assemblies on Cu (111) Induced by Indirect Coupling through the Substrate'*J. P. Pierce, M.A. Torija, Z. Gai, Junren Shi, T.C. Schulthess, G.A. Farnan, J. F. Wendelken, E.W. Plummer, and J. Shen, Phys. Rev. Lett. 92, 237201 (2004).

4.12 *'Buffer-Layer-Assisted Growth of Nanocrystals: Ag-Xe-Si(111)'*F. Huang et al., Phys. Rev. B 49, 3962 (1994).

Chapter 5

5.1 "*Tailoring magnetism in artificially structured materials: the new frontier"* J. Shen and J. Kirschner, Surf. Sci. 500, 300 (2002).

5.2 '*Direct Observation of Internal Spin Structure of Magnetic Vortex Cores"* A. Wachowiak, J. Wiebe, M. Bode, O. Pietzsch, M. Morgenstern, and R. Wiesendanger, Science 298, 577 (2002).

5.3 "*An inverse transition of magnetic domain patterns in ultrathin film" s*O. Portmann, A. Vaterlaus, and D. Pescia, Nature (London) 422, 701 (2003).

5.4 "*Magnetic live surface layers in Fe/Cu(100)"* J. Thomassen F. May, B. Feldmann, M. Wuttig, and H. Ibach., Phys. Rev. Lett. 69, 3831 (1992).

5.5 "*Magnetic phases of ultrathin Fe grown on Cu(100) as epitaxial wedges"* D. Q. Li, M. Freitag, J. Pearson, Z. Q. Qiu, and S. D. Bader, Phys. Rev. Lett. 72, 3112 (1994).

5.6 "*Growth and morphology of ultrathin Fe films on Cu(001)"* J. Giergiel, J. Shen, J. Woltersdorf, A. Kirilyuk, and J. Kirschner, Phys. Rev. B 52, 8528 (1995).

5.7 "*Mössbauer Effect Study of Magnetism and Structure of fcc-like Fe(001) Films on Cu(001)"* R. D. Ellerbrock, A. Fuest, A. Schatz, W. Keune, and R. A. Brand, Phys. Rev. Lett. 74, 3053 (1995).

5.8 "*Surface Magnetism of Ultrathin gamma -Fe Films Investigated by Nonlinear Magneto-optical Kerr Effect"* M. Straub, R. Vollmer, and J. Kirschner, Phys. Rev. Lett. 77, 743 (1996).

5.9 "*Total Energy Spectra of Complete Sets of Magnetic States for fcc-Fe Films on Cu(100)"* T. Asada and S. Blugel, Phys. Rev. Lett. 79, 507 (1997).

5.10 "*Nucleation of bcc Iron in Ultrathin fcc Films"* A. Biedermann, M. Schmid, and P. Varga, Phys. Rev. Lett. 86, 464 (2001).

5.11 "*Spin-Density Wave in Ultrathin Fe Films on Cu(100)"* D. Qian, X. F. Jin, J. Barthel, M. Klaua, and J. Kirschner, Phys. Rev. Lett. 87, 227204 (2001).

5.12 "*Temperature Dependence of the Surface Anisotropy of Fe Ultrathin Films on Cu(001)"* A. Enders, D. Peterka, D. Repetto, N. Lin, A. Dmitriev, and K. Kern, Phys. Rev. Lett. 90, 217203 (2003).

5.13 "*Structural and magnetic phase transitions of Fe on stepped Cu(111)"* J. Shen, M. Klaua, P. Ohresser, H. Jenniches, J. Barthel, Ch. V. Mohan, and J. Kirschner., Phys. Rev. B 56, 11 134 (1997).

5.14 *Magnetic Moment of fcc Fe(111) Ultrathin Films by Ultrafast Deposition on Cu(111)* J. Shen P. Ohresser, Ch. V. Mohan, M. Klaua, J. Barthel, and J. Kirschner., Phys. Rev. Lett. 80, 1980 (1998).

5.15 "*Magnetism of nanostructures studied by x-ray magnetic circular dichroism: Fe on Cu(111)"* P. Ohresser, G. Ghiringhelli, O. Tjernberg, and N. B. Brooks, Phys. Rev. B 62, 5803 (2000).

5.16 "*Diffusion-Limited Aggregation, a Kinetic Critical Phenomenon"* T. A. Witten and L. M. Sander, Phys. Rev. Lett. 47, 1400 (1981).

5.17 "*Dynamic Scaling of Growing Interfaces"* M. Karder, G. Parisi, and Y. C. Zhang, Phys. Rev. Lett. 56, 889 (1986).

5.18 "*Kinetic surface roughening. II. Hypercube-stacking models"* L. H. Tang, B. M. Forrest, and D. E. Wolf, Phys. Rev. A 45, 7162 (1992).

5.19 "*Growth and structure of Fe and Co thin films on Cu(111), Cu(100), and Cu(110): A comprehensive study of metastable film growth"* M. T. Kief and W. F. Egelhoff, Phys. Rev. B 47, 10785 (1993).

5.20 "*Magnetovolume instabilities and ferromagnetism versus antiferromagnetism in bulk fcc iron and manganese "* V. L. Morizzi, P. M. Markus, and J. Kubler, Phys. Rev. B 39, 6957 (1989).

Chapter 6

6.1. *Surface State Scattering at a Buried Interface,* F. Schiller, R. Keyling, E. V. Chulkov, and J. E. Ortega, Phys. Rev. Lett. 95, 126402 (2005)\

6.2. *Photoemission of a Quantum Cavity with a Nonmagnetic Spin Separator* C. Koitzsch, C. Battaglia F. Clerc, L. Despont, M. G. Garnier, and P. Aebi1, Phys. Rev.Lett. 95, 126401 (2005)

6.3. *Direct measurements of the L-gap surface states on the „111... face of noble metals by photoelectron spectroscopy* F. Reinert, G. Nicolay, S. Schmidt, D. Ehm, and S. Hufner, Phys. Rev. B, 63, 115415 (2001)

6.4. *Tunneling into a Single Magnetic Atom: Spectroscopic Evidence of the Kondo Resonance,* V. Madhavan, W. Chen, T. Jamneala, M. F. Crommie, and N. S. Wingreen Science, 280,5363 (1998)

6.5. *Kondo Scattering Observed at a Single Magnetic Impurity,* Jiutao Li and Wolf-Dieter Schneider,Richard Berndt, Bernard Delley Phys. Rev. Lett. 80, 28

APPENDIX

A.1. Novel measurements in Fe nanodots assemblies: surface states role

It has been demonstrated that the novel magnetic interaction is connected to the Cu(111) surface and not with metallicity. Surface states are a distinctive characteristic of this substrate. In an attempt to identify if surface states are the origin of the novel interaction, we performed two more experiments.

We modified the Cu(111) surface to increase the roughness. After cleaning the surface, the Cu was sputtered for 30 minutes. STM images confirmed that surface states were no longer detectable. Critical temperatures were compared (fig A.1) for smooth versus rough surface. The critical temperature was higher when surface states were present for any dot distribution.

In the second experiment (fig A.2) we attempted to eliminate the surface states by adding 8 ML of Cu. In this case, the critical temperature decreased after the capping. This has provided more evidence to identify the novel interaction with the presence of surface states in the Cu (111) surface.

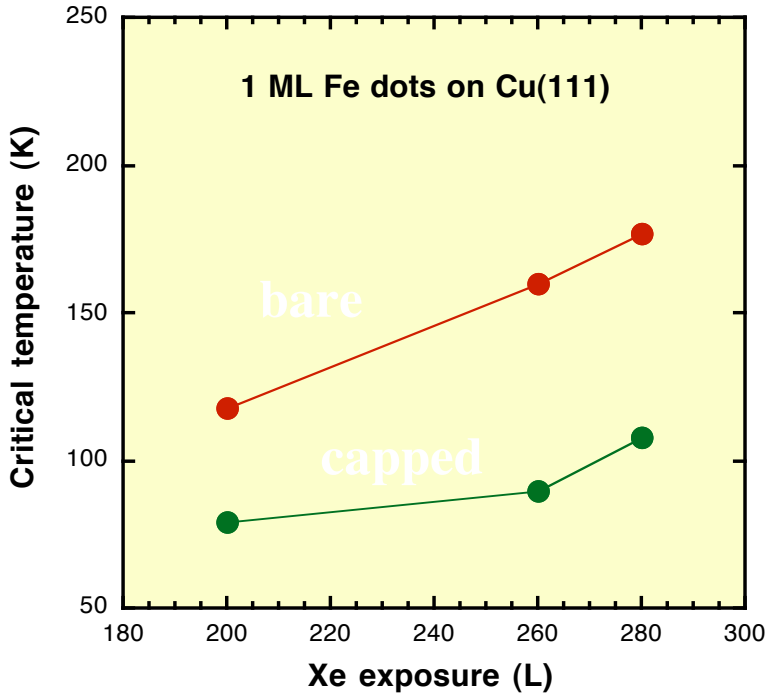

Figure A1.1 Critical temperatures for when the array was uncapped and capped by 12 ML.

The naked surface has a more stable magnetism.

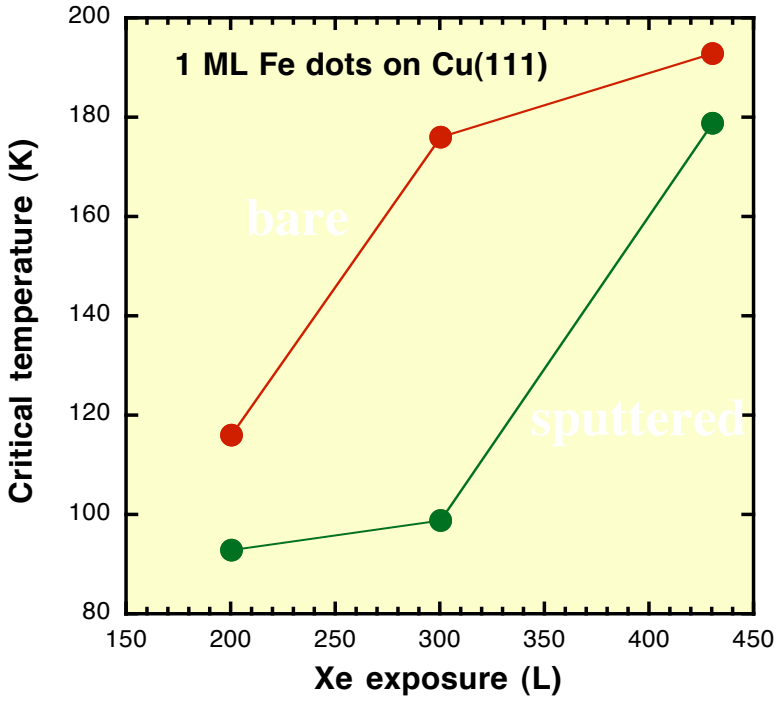

Figure A1.2 Diference in critical temperature due to the quality of the surface.

The magnetism is more stable for samples that have a smooth surface.

A.2. Ferromagnetic Nanocrystals of Antiferromagnetic FeGe

This chapter is based on an article submitted to Phys. Rev. Lett. The magnetic behavior of FeGe nanostructures grown on Ge(111) was analyzed. The ferromagnetism observed in the bulk antiferromagnet was due to the lattice distortion in the epitaxially grown nanowires. My contribution to the article consists on the MOKE characterization of the nanowires.

Changgan Zeng, [1] P. R. C. Kent,[2] M. Eisenbach,[3] G. M. Stocks, [3] Maria Torija,[1] Jian Shen,[4, 1] and Hanno H. Weitering [1, 4]

1Department of Physics and Astronomy, The University of Tennessee, Knoxville, Tennessee 37996

2The University of Tennessee, Knoxville, Tennessee 37996

3Metals and Ceramics Division, Oak Ridge National Laboratory, Oak Ridge, TN 37831

4Condensed Matter Sciences Division, Oak Ridge National Laboratory, Oak Ridge, TN 37831 (Dated: May 24, 2005)

Epitaxial nano-crystals of FeGe have been stabilized on Ge(111). The nano-crystals assume a quasi one-dimensional shape as they grow exclusively along the <1 $\bar{1}$0> direction of the Ge(111) substrate, culminating in the monoclinic modification of FeGe. The uni-directional growth results from a close match between the Ge-atom spacing along <1 $\bar{1}$0> Ge and monoclinic b-axis of FeGe. Whereas monoclinic FeGe is

antiferromagnetic in the bulk, the nanocrystals are surpisingly strong ferromagnets below ~250 K with an average magnetic moment of 0.8 μB per Fe atom. Density functional calculations demonstrate that volume ferromagnetism is stabilized by a small strain along the growth direction of the nano-crystals.

Magnetism and structure are strongly intertwined [1, 2], particularly in nanoscale systems [3, 4]. As a rule of thumb, an increasing lattice constant enhances the magnetic moment and potentially stabilizes ferromagnetic ordering. Both properties are highly desirable for applications. To increase the lattice constant of a low-dimensional or nanoscale structure, the most common approach is to epitaxially stabilize a magnetic film on a suitable substrate. Unfortunately, the increase of the lattice parameter is usually limited by epitaxial strain relaxation and is rarely sufficient to form new magnetic phases. Interesting exceptions include epitaxially grown fcc Fe films on Cu, which exhibit a range of magnetic phases including antiferromagnetism, low-spin ferromagnetism, and high-spin ferromagnetism upon a small variation of the lattice parameter of the Fe films [5].

In this Letter, we report on a novel nanophase material that is ferromagnetic at the nanoscale (Tc ~ 250 K) while being antiferromagnetic in the bulk, namely FeGe on Ge(111). Bulk FeGe exhibits an interesting variety of structures and magnetic properties[6–8]. It crystallizes in three different polymorphs. The cubic polymorph is an antiferromagnetic metal with a Dzyaloshinskii-Moriya type spin spiral [6] while the hexagonal [7] and monoclinic [8] polymorphs exhibit complex, modulated spin structures with a net antiferromagnetic magnetization. The FeGe nanocrystals, on the other hand,

appear to be strongly ferromagnetic. Their structure and shape gradually evolves as a function of annealing temperature, culminating in the formation of long nanowires that can be identified as the monoclinic polymorph of FeGe. We find that the Ge(111) substrate plays a key role in stabilizing ferromagnetism in monoclinic FeGe. The substrate not only serves as a template for uni-directional growth but also imposes a small tensile strain along the growth direction of the nanocrystals. Density functional calculations demonstate that this tips the delicate balance of competing exchange interactions into a collective ferromagnetic response. These FeGe nanoparticles present a first example of volume ferromagnetism in nanoparticles of an antiferromagnetic compound.

Experiments were carried out in two different UHV systems equipped with thermal effusion sources. One UHV system was furthermore equipped with a Scanning Tunneling Microscope (STM) and monochromatic X-ray photoelectron spectroscopy (XPS) while the other system has capabilities for in situ magneto-optical Kerr effect (MOKE) measurements and Auger Electron spectroscopy. Ge(111) substrates were cleaned in-situ by Neion sputtering and annealing to 650 ◦C. FeGe nanocrystallites were produced by depositing Fe onto Ge(111) and subsequent annealing for about ten minutes. The Fe coverage in both experiments was determined via ex-situ Rutherford Backscattering Spectrometry (RBS), which measures the absolute Fe coverage [9]. Samples characterized with STM were subsequently capped with a 20 nm-thick amorphous Ge film for ex-situ magnetic measurements with a SQUID magnetometer.

The evolution of the surface morphology was studied as a function of annealing temperature between 0.3 to 2.0 ML of Fe. In this coverage range, the morphology does not depend on coverage. The annealing temperature is very critical, however. Fig. A.2.1(a) shows the STM image of the surface morphology after deposition of 2 ML of Fe on Ge(111). The Fe atoms aggregate into small "baby clusters". The structure and composition of these clusters cannot be determined from STM imaging. MOKE measurements in Fig. A.2.1(b) reveal a ferromagnetic hysteresis loop with an easy axis of magnetization that is perpendicular to the film. Crystallites with a well defined, elongated shape form after annealing to 460 ◦C, as is shown in Fig. 1(c). Their identity is neither obvious but we notice that Fe on Si(111) produces nanocrystallites of identical appearance [10]. Those crystallites had been identified as cubic FeSi having the because of a better lattice match [11]. Similar arguments can be made for FeGe on Ge(111) and accordingly we tentatively attribute the crystallites in Fig. A.2.1(c) to c-FeGe. The crystallites are ferromagnetic but the Kerr response is weaker while easy axis of metastable CsCl structure (c-FeSi). Although bulk FeSi crystallizes in the simple-cubic B20 structure (ε-FeSi), the CsCl modification can be stabilized epitaxially on Si(111) magnetization has changed to in-plane; Fig. A.2.1(d). Still higher annealing temperature leads to longer nanocrystallites and vanishing Kerr response. Figure A.2.1(e) shows the morphology after annealing to 620 ◦C. The surface is covered with long "nanowires" that are aligned along the three equivalent <1 $\bar{1}$0> directions of the Ge substrate. They average 165 nm in length, 6 nm in width, and 1.0 nm in height. Fig. A.2.2(a) shows a close-up image of the nanocrystals at 0.3 ML. The lower coverage exposes the substrate

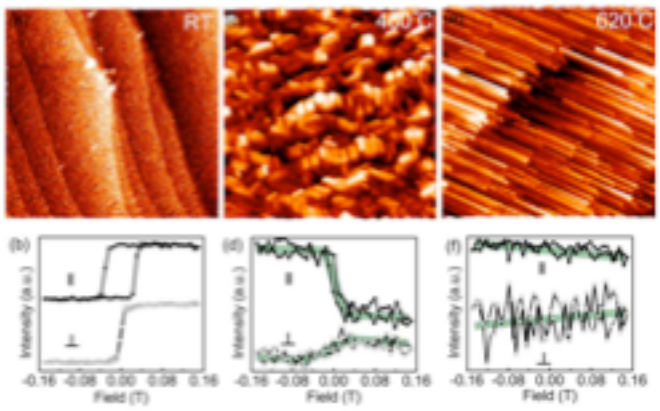

Figure A.1.1. STM images (500 nm × 500 nm) (top) and corresponding MOKE data (bottom) of Fe or iron-germanide nanocrystals on Ge(111).

The Fe coverage is 2 ML and MOKE data were recorded at 77 K. Annealing temperatures and magnetic field orientations are indicated.

and allows us to resolve the individual atoms of the Ge(111)-c(2×8) substrate in between the nanocrystallites. Interestingly, the nanocrystals grow across the terrace steps and can even cross one another.

This remarkable uni-directional growth of the nanocrystals indicates one-dimensional lattice matching along the Ge<1 $\bar{1}$0> direction. Although a novel germanide nanophase cannot be ruled out, we first look for bulk phases that would match the Ge(111) substrate along the <1 $\bar{1}$0> direction, which has a repeat distance of 4.00 Å. All possible Fe-Ge comounds are listed in Ref. 12, along with their lattice constants and magnetic properties. Considering only the lattice constants, several of these phases would be good candidates for epitaxial growth on Ge(111). For instance, cubic ε-FeGe (a = 4.70 Å) and metastable c-FeGe could possibly be stabilized on Ge(111) with a lattice mismatch of the order of 5% or less, as is the case of FeSi on Si(111) [11]. The hexagonal (0001) basal plane of Fe5Ge3 (a = 4.02 Å and c = 5.02 Å) matches the Ge(111) substrate within 0.5% but this would not explain uni-directional growth. The only viable candidates for uni-directional growth are bcc Fe (a = 2.87 Å), hexagonal FeGe (a = 5.00 Å and c = 4.06 Å), and monoclinic FeGe (a = 11.84 Å, b = 3.94 Å, c = 4.94 Å, and β =103.51 ◦). Each of these crystal structures would match the Ge lattice spacing along the <1 $\bar{1}$0> direction to 1.5% or less while having a larger mismatch orthogonal to <1 $\bar{1}$0> Ge. It is inconceivable that Fe and Ge would not form an alloy at 700 ◦C [12, 13]. Fe 2p XPS core level spectra taken before and after annealing indeed suggest alloy formation (not shown). Fig. A.2.2(b) and (c) show close-up STM images taken from the FeGe nanocrystals. Although atomic resolution could not be acquired in our experiments, the

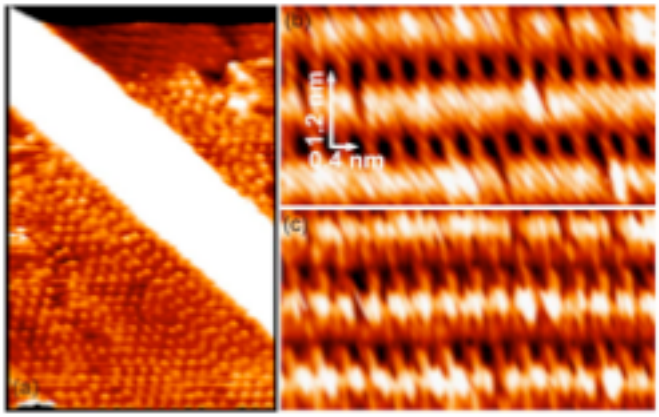

Figure A.2.2. (a) Close-up 30 nm × 30 nm STM image of a FeGe nanowire.

It is showing atomic resolution from the Ge(111)-c(2×8) substrate (Vs = 1.0 V); (b) and (c) are nearly atomic-resolved STM images of a monoclinic FeGe nanocrystal, recorded in and magnetic field orientations are indicated. in the dual bias mode with Vs of -1.0 V (a) and +1.0 V (b).

unit cell dimensions can be determined easily. The dimensions are 4 Å × 12 Å and correspond to the unit cell parameters in the (a, b) plane of monoclinic FeGe [8]. The end phase of the annealing series is therefore identified as monoclinic FeGe. The quasi one-dimensional growth is attributed to the very small lattice mismatch between the monoclinic b-axis of FeGe and the <1 $\bar{1}$0> direction of Ge (1.5%). The morphological evolution of the nanoscrystals with annealing temperature (Fig. A.2.1) is also consistent with the temperature dependence of the bulk phases. FeGe evolves from cubic to hexagonal, and finally monoclinic as the annealing temperature is raised; the bulk monoclinic phase is formed above 740 ◦C [13].

The morphological evolution of the nanocrystals is accompanied by the initial reorientation of the magnetization and gradual reduction of the Kerr response (Fig. A.2.1). To further investigate the origin of the reduced Kerr response, we performed ex-situ SQUID measurements on capped and uncapped samples with a total Fe coverage of 2.0 ML. The capping layer consists of 200 Å of amorphous Ge, deposited at room temperature, and complete burial was verified with XPS and STM. SQUID results are identical for the capped and uncapped samples, showing that the FeGe nanocrystals are stable against capping and oxidation. Interestingly, the ferromagnetic saturation moment from SQUID, measured at 5 K, depends on the annealing temperature and evolution stage of the moment drops below the detection limit of MOKE. The inset of Fig. A.2.3 shows ferromagnetic hysteresis loops of the monoclinic nanophase crystals measured with SQUID, following a high temperature anneal at 700 ◦C (diamagnetic background subtracted). The average saturation moment per Fe atom is 0.8 μB at 5 K. The

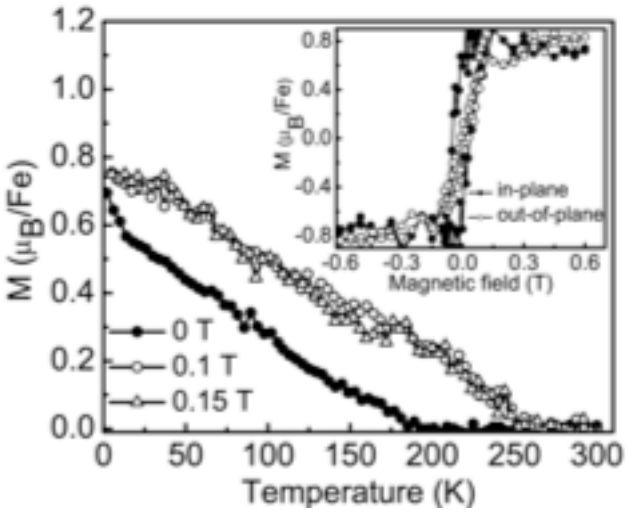

Figure A.2.3. SQUID measurements of 2 ML Fe on Ge(111), annealed to 700 ◦C.

Remanent and field-induced magnetizations as a function of temperature. All measurements were taken with in-plane magnetic field. The inset shows field-dependent magnetization at T = 5 K, showing clear evidence of ferromagnetism. low the Kneel temperature of 279 K.

magnetization of the monoclinic nanocrystals is also shown as a function of temperature in Fig. A.2.3. Remanence vanishes near 200 K while the field-induced moment disappears near 250 K, which is slightly above the ferromagnetic Curie temperature.

Ferromagnetism in nanoparticles of antiferromagnetic materials is usually attributed to uncompensated spins at the surface or interface of the nanoparticle, as originally proposed by N´eel [14]. Alternatively, Mørup and Fransdsen [15] recently argued that magnetic sublattices in antiferromagnetic nanostructures precess in such a way that the moments are not exactly antiparallel, resulting in a net magnetization that increases with temperature. Either way, the net magnetization is expected to be very small. For instance, NiO and CoO nanoparticle systems have remanent moments that are smaller than 0.1 μB [16, 17]. Ferromagnetism in FeGe nanoparticles, on the other hand nanocrystals. For instance, the magnetic moment per Fe atom at 5 K is 1.5 ± 0.2 μB when the Fe deposit is annealed at 460 ◦C, 0.9 ± 0.2 μ_B when annealed at 620 ◦C, and 0.8 ± 0.2 μ_B when annealed at 700 ◦C. This observation is consistent with the gradual weakening of the Kerr signal (Fig. A.2.1). Eventually, the magnetic FeGe nanoparticles is possibly related to nano confinement. However, since the height and width of the nanoparticles are not easily tunable, it will be difficult to establish such a relationship on the basis of experiments. Instead, we conjecture that ferromagnetism in FeGe nanoparticles can be explained on the basis of the peculiar electronic structure of bulk FeGe and related compounds [18–20]. For instance, cubic FeGe is an antiferromagnetic metal with a Dzyaloshinskii-Moriya spiral spin structure with a period of 683 to 700 Å below the N

´eel temperature of 279 K [6]. The length of the spiral makes this compound almost ferromagnetic. Iso-structural FeSi, on the other hand, is a nonmagnetic, small-band gap semiconductor, sometimes referred to as a Kondo insulator [18]. The $FeSi_{1-x}Ge_x$ solid solution undergoes a transition from Kondo insulator to metallic metal at $x \sim 0.3$ [19]. Finally, electronic structure calculations indicate that FeGe becomes a nonmagnetic semiconductor under pressure [20]. All of these observations suggest that the band gap and magnetic properties are very sensitive to strain, at least for the cubic ε-FeGe phase. Here, we consider the effect of a-b plane strain due to epitaxy on the monoclinic phase.

To investigate the influence of strain we performed ab-initio projector-augmented wave (PAW) density functional calculations [21] for the 16 atom unit cell monoclinic structure. For bulk calculations we utilized a well-converged 25 Ry plane-wave cutoff and 4 × 8 × 8 Monkhorst-Pack k-point grid for tetrahedral Brillouin zone integration. Lattice vectors were relaxed until the external pressure was 1 kBar or less. Due to the many potential antiferromagnetic ground states we performed a combinatoric search over all 1680 potential configurations: the lowest energy antiferromagnetic configuration consists of layers of a-b plane upspin-downspin Fe pairs. For the relaxed bulk monoclinic structure we find a delicate balance between ferromagnetism and antiferromagnetism: within GGA [22] antiferromagnetism is favored by 0.016 eV/cell, while in LDA [23] ferromagnetism is favored by 0.091 eV/cell. GGA calculations using a larger 6×12×12 k-point grid again favor antiferromagnetism by 0.015 eV/cell. The average calculated moment of the ferromagnetic phase is 1.4 μ_B per Fe atom, with individual moments 1.0(x2), 1.5(x2), and 1.8 (x4) μ_B.

To establish the possible role of epitaxial strain in stabilizing ferromagnetism we surveyed the electronic structure as a function of epitaxial conditions, varying in-plane a and b lattice vectors, and fully relaxing all atomic positions and the c-axis. For efficiency we held the monoclinic angle fixed and used a 2x2x4k – point grid. In Fig. A.2.3 we show the calculated difference in antiferromagnetic and ferromagnetic total energies as a function of the in-plane lattice constants. The contours and lowest energy configurations were obtained froma10x6gridof calculations. This data shows that the magnetic ground state of FeGe depends sensitively on the lattice constants: compression along the a axis and expansion along the b axis favor ferromagnetism, while the overall energy scale is small. The sensitivity to the in-plane lattice constants is consistent with the calculated a-b plane spin pairings in the antiferromagnetic configuration. There is no substantial change in e.g. the energy of specific d orbitals or features in the density of states with epitaxy: ferromagnetism results from a multitude of changes to the electronic structure of FeGe with strain.

Our theoretical results suggest that epitaxial strain is the underlying reason for ferromagnetism in the FeGe nanocrystals: expansion along b to lattice match Ge <1 10> (4.00 Å) produces ferromagnetism if the aaxis is simultaneously compressed to~11.55 Å or smaller, a ~2% strain.

In conclusion, FeGe has been stabilized on Ge(111) in the form of nanocrystals. Their structure and shape gradually evolves as a function of annealing temperature, culminating in the formation of long nanowires of the monoclinic polymorph of FeGe. The positive identification of monoclinic FeGe presents first example of volume

ferromagnetism in nanoparticles of an antiferromagnetic compound. magneto-structural properties of FeGe. These findings show that the complexity of competing interactions in some bulk materials can lead to surprising and potentially useful properties in the corresponding nanophase. This work is funded by NSF under contract No. DMR 0306239(FRG). This research used computational resources of the Center for Computational Sciences, and was sponsored by the offices of Basic Energy Sciences andAdvanced Scientific Computing Research, U.S. Department of Energy. Oak Ridge National Laboratory is managed by UT-Battelle, LLC, for the U.S. Department of Energy under contract No. DE-AC05-00OR22725.

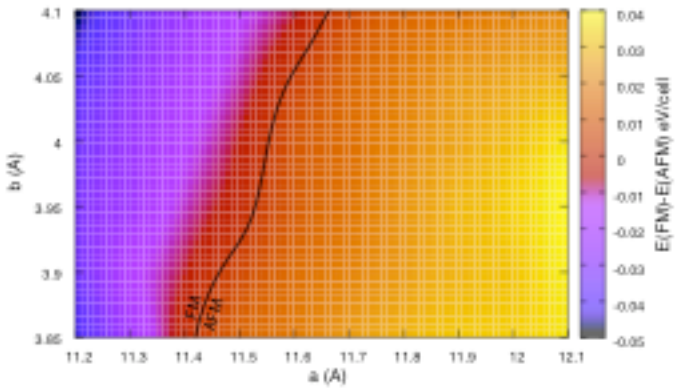

Figure A.2.4. Calculated energy difference between ferromagnetic and antiferromagnetic ground states of monoclinic FeGe.

The approximate zero-energy difference contour is shown.

Calculations suggest that ferromagnetism in these materials is stabilized by epitaxial strain. This unexpected ferromagnetism can be traced to the rich and intriguing

References A.2.

A.2.1“Ultrafast Generation of Ferromagnetic Order via a Laser-Induced Phase Transformation in FeRh Thin Films” Ganping Ju, Julius Hohlfeld, Bastiaan Bergman, René J. M. van de Veerdonk, Oleg N. Mryasov, Jai-Young Kim, Xiaowei Wu, Dieter Weller, and Bert Koopmans., Phys. Rev. Lett. 93, 197403(2004).

A.2.2 S. Yuasa et al., J. Phys. Soc. Jpn. 64, 4906(1995).

A.2.3 “Tailoring magnetism in artificially structured materials: the new frontier” J. Shen and J. Kirschner, Surf. Sci. 500, 300 (2002).

A.2.4 “Magnetism in low dimensionality” S.D. Bader, Surf. Sci. 500, 172(2002).

A.2.5 “Growth and morphology of ultrathin Fe films on Cu(001)” J. Giergiel, J. Shen, J. Woltersdorf, A. Kirilyuk, and J. Kirschner J, Phys. Rev. B 52, 8528(1995);

“Mössbauer Effect Study of Magnetism and Structure of fcc-like Fe(001) Films on Cu(001)” R. D. Ellerbrock, A. Fuest, A. Schatz, W. Keune, and R. A. Brand., Phys. Rev. Lett. 74, 3053(1995);

“Surface Magnetism of Ultrathin gamma -Fe Films Investigated by Nonlinear Magneto-optical Kerr Effect” M. Straub, R. Vollmer, andJ. Kirschner, Phys. Rev. Lett. 77, 743(1996);

“Total Energy Spectra of Complete Sets of Magnetic States for fcc-Fe Films on Cu(100)” T. AsadaandS. Blugel, Phys. Rev. Lett. 79, 507(1997);

“Nucleation of bcc Iron in Ultrathin fcc Films” A.Biedermann,M.Schmid,and P.Varga, Phys. Rev. Lett. 86, 464(2001);

"Spin-Density Wave in Ultrathin Fe Films on Cu(100)" D. Qianet al., Phys. Rev. Lett. 87, 227204(2001); A. Enders et al., Phys. Rev. Lett. 90, 217203(2003).

A.2.6 "Magnetic structures of cubic FeGe studied by small-angle neutron scattering" B. Lebech, J. Bernhard, andT. Freltoft, J. Phys.: Condens. Matter. 1, 6105(1989).

A.2.7 "Neutron diffraction studies of the low-temperature magnetic structure of hexagonal FeGe" J. Bernhard, B. Lebech, andO. Beckman, J. Phys. F: Met. Phys. 14, 2379(1984).

A.2.8 "Magnetic structures of monoclinic FeGe" G.P. Felcher, J.D. Jorgensen, and R. Wappling, J. Phys. C: SolidStatePhys. 16, 6281(1983).

A.2.9 In our definition, one monolayer corresponds to the atomic density in the (110) plane of bcc Fe.

A.2.10 "Thermal reaction of iron with a Si(111) vicinal surface: Surface ordering and growth of CsCl-type iron silicide" A. Wawro, S. Suto, R. Czajka and A. Kasuya1., Phys. Rev. B 67, 195401(2003).

A.2.11 "Structural and electronic properties of metastable epitaxial FeSi1+x films on Si(111)" H. von Känel, K. A. Mäder, E. Müller, N. Onda, and H. Sirringhaus Phys. Rev. B45, 13807(1992).

A.2.12 "Magnetic Properties of Metals" H.P.J. Wijn, (Springer Verlag, Berlin Heidelberg, 1991), p. 154.

A.2.13 , "Phase Diagrams of Binary Iron Alloys" E. Kato, andS. Nunoue, edited by H. Okamoto (ASMInternational, 1993), p. 159.

A.2.14 L. N′eel, in LowTemp. Phys., edited by C. Dewitt, B. Dreyfus, and P.D. deGennes (GordonandBeach, New York, 1962), p. 413.

A.2.15 “Thermoinduced Magnetization in Nanoparticles of Antiferromagnetic Materials” S. Mørup, and C. Frandsen, Phys. Rev. Lett. 92, 217201 (2004).

A.2.16 “Magnetic anomalies in NiO nanoparticles” Salah A. Makhlouf, F. T. Parker, F.E. Spada, and A. E. Berkowitz., J. Appl. Phys. 81, 5561(1997); “Finite Size Effects in Antiferromagnetic NiO Nanoparticles” R.H. Kodama, and S.A.Makhlouf, Phys. Rev. Lett. 79, 1393(1997).

A.2.17 “Finite size effects on the moment and ordering temperature in antiferromagnetic CoO layers” Y. J. Tang, David J. Smith, B. L. Zink, F. Hellman, and A. E. Berkowitz Phys. Rev. B67, 54408(2003).

A.2.18 “First-Order Transition between a Small Gap Semiconductor and a Ferromagnetic Metal in the Isoelectronic Alloy FeSi1–xGex” V. I. Anisimov, R. Hlubina, M. A. Korotin,V. V. Mazurenko, T. M. Rice, A. O. Shorikov, and M. Sigrist1., Phys. Rev. Lett. 89, 257203(2002).

A.2.19 “First-Order Transition between a Small Gap Semiconductor and a Ferromagnetic Metal in the Isoelectronic Alloy FeSi1–xGex” S. Yeo, S. Nakatsuji, A. D. Bianchi, P. Schlottmann,3 Z. Fisk, L. Balicas, P. A. Stampe, and R. J. Kennedy Phys. Rev. Lett. 91, 046401(2003).

A.2.20 “Electronic structure and magnetism of FeGe with B20-type structure” H. Yamada, K. Terao, H. Ohta and E. Kulatov., Physica B 329-333, 1131(2003).

A.2.21.” From ultrasoft pseudopotentials to the projector augmented-wave method, Kresse and D. Joubert, Phys.Rev.B 59, 1758 (1999); “Ab initio molecular dynamics for liquid metals”. Kresse and J. Hafner, ibid. 47, 558(1993); “Ab initio molecular-dynamics simulation of the liquid-metal–amorphous-semiconductor transition in germanium”,.ibid 49, 14251 (1994).

A.2.22. “Atoms, molecules, solids, and surfaces: Applications of the generalized gradient approximation for exchange and correlation”,John P. Perdew ,J. A. Chevary and S. H. Vosko, Koblar A. Jackson, Mark R. Pederson, and D. J. Singh, Carlos Fiolhais , Phys. Rev. B46, 6671(1992).

A.2.23. “Self-interaction correction to density-functional approximations for many-electron systems”, J. P. Perdew and A. Zunger. Phys. Rev. B23, 5048 (1981).

A.3: Identification of FeGe stochiometry and crystal structure by HRTEM. Courtesy of M. Varela

Measurements conducted after article submission have made it possible to image and confirm the structure of FeGe nanowires. A sample annealed to 720 and capped by xxx, was analyzed in the HRTEM combined with EELS.

The atomic ratio of Fe to Ge was 1:1 in the wires, and there were no traces of Fe in the Ge substrate (fig B.1). The lattice parameters (inset fig A3.1) corresponded to a distorted tetragonal cell. The two different patterns observed were the same phase with different orientations. The interface was clean and without visible intermixing.

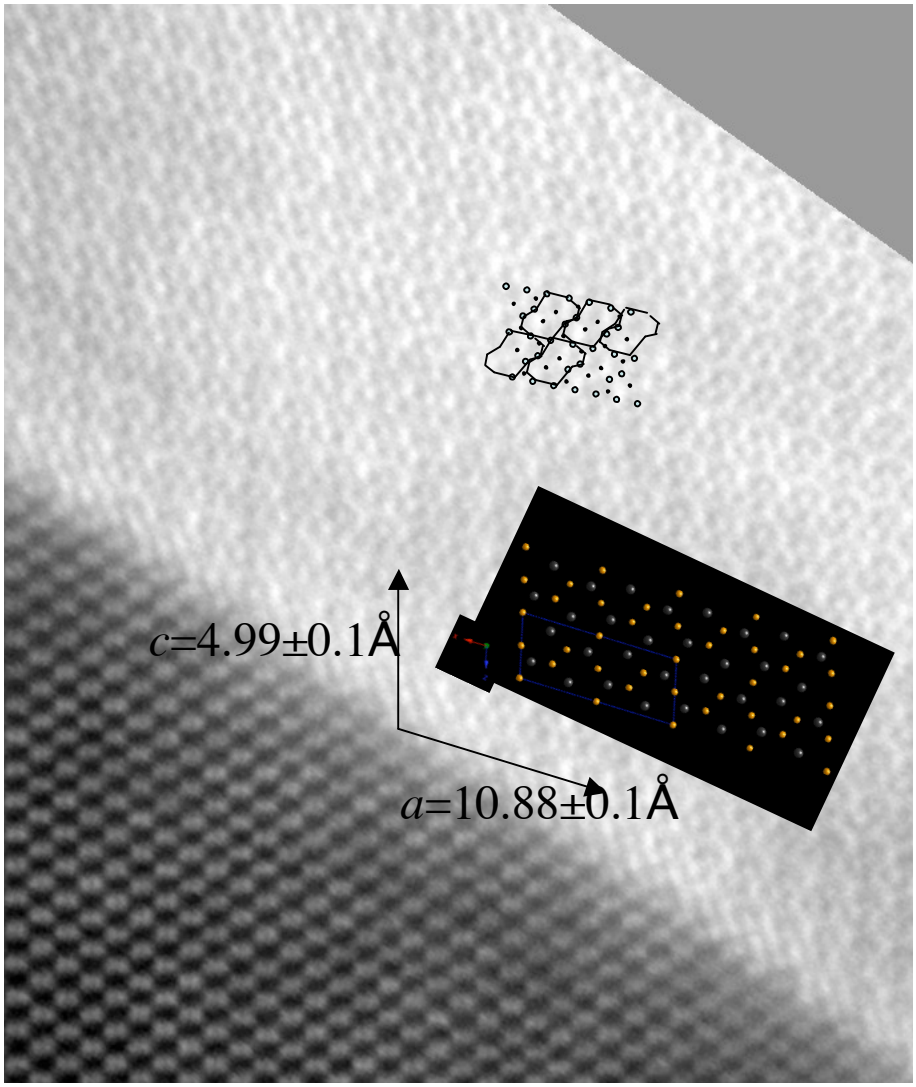

Figure A.3.1 Monoclininc phase of FeGe wires

The a-axis seems to be rotated about 16 degrees off the interface plane. It lies perpendicular to the wire long axis.The picture in the black inset is the crystal structure. The blue square shows the unit cell in this projection [0-40] The b axis is in plane. The a-axis is slightly compressed, while the c axis is slightly expanded. Assuming that the b axis is matching the substrate in plane lattice constant (3.94 Å), the unit cell volume is approximately (214±15) Å3

A.4. Theoretical principles in the Magneto-Optical Kerr Effect

In the middle of the XIX century when it was established that a linearly polarized light beam that is transmitted or reflected on a magnetic material could generate ellipticity. The phenomenon of transmission is called Faraday effect, and Kerr effect is the related one to the reflexion.

The MOKE effect has had a huge impact in technology because it was the first phenomena to be used in recording magnetic media, MO disk, in the old computers. In the last 20 years, the Surface Magneto Optical Kerr effect has become an indispensable tool to detect magnetism because its great sensitivity allows the detection of magnetic materials under the monolayer regime. The physical origin would be explained ahead, and practical details will presented later on.

The first concept to explain in this phenomenon is the difference in light polarization. Linearly polarized light travels in the direction z and is made of two electromagnetic waves whose electric vectors are perpendicular to the propagation direction and in phase with each other. In the circularized polarization, the two vectors are out of phase ¼. It is possible then, to study the linear polarized light like a composition of two circularized polarized beam with opposite phase, right and left handed.

Anisotropies in the conductivity tensor, such as magnetic field, can change the phase difference between left and right circular light.

$$\begin{pmatrix} J_x \\ J_y \\ J_z \end{pmatrix} = \begin{pmatrix} \sigma_{xx} & \sigma_{xy} & \sigma_{xz} \\ \sigma_{yx} & \sigma_{yy} & \sigma_{yz} \\ \sigma_{zx} & \sigma_{zy} & \sigma_{zz} \end{pmatrix} \begin{pmatrix} E_x \\ E_y \\ E_z \end{pmatrix}$$

Intuitively, the diagonal elements connect the light and the medium, and the terms that relate two different directions lead to indices of refraction for right and left-circular polarized light in a medium. These no-diagonal elements are responsible for magneto optical effects.

As a example, if two non-iagonal elements are not null, and because of symmetry requirements equal and opposite, and the medium is isotropic:

$$\sigma_{xy} = -\sigma_{yx}$$

$$\sigma_x = \sigma_y = \sigma_z$$

And considering the Maxwell equations applied to plane waves:

$$\nabla \times H = \frac{1}{c}\frac{\partial E}{\partial t} + \frac{4\pi}{c}\sigma \bullet E$$

Taking the curl in both sides and substituting E by a wave propagating in the z direction.

$$E = \begin{pmatrix} E_x \\ E_y \\ E_z \end{pmatrix} e^{i\omega t - \frac{i\omega N}{c} z}$$

Focusing on equations on the x and y components in the electrical field, it is possible to have two equations that relate the two different elements with the N parameter. And from then, there are two modes. One for right left handed and right handed.

$$\begin{pmatrix} \frac{\omega^2 N^2}{c^2} E_x \\ \frac{\omega^2 N^2}{c^2} E_y \\ 0 \\ \end{pmatrix} e^{i\omega t - \frac{i\omega N}{c} z} = -\frac{(i\omega)^2}{c^2} \begin{pmatrix} E_x \\ E_y \\ E_z \end{pmatrix} e^{i\omega t - \frac{i\omega N}{c} z} - \frac{4\pi}{c^2} \begin{pmatrix} \sigma_0 E_x - \sigma_1 E_y \\ \sigma_1 E_y - \sigma_0 E_x \\ \sigma_0 E_z \end{pmatrix} e^{i\omega t - \frac{i\omega N}{c} z}$$

The basic explanation for the magneto-optical effect is the intimate relationship between the electrons of the magnetized solids.

The microscopic origin of the magneto-optical effect is connected with the Lorentz force that electrons in the magnetized solid induce in the photons.

This simple picture doesn't explain well the reason ferromagnetic materials have such a strong Kerr effect, because the internal field is not strong. One of the possible explanations includes the interaction of an electron and the effective field that fields lead to the non-zero diagonal elements.

The term of the spin orbit terms incorporates the electron magnetic moment and the effective field when this electron is moving with moment p through an electrical field

in the material. The non-diagonal elements show up in the conduction equation as the element that will create the ellipticity.

Vita.

Maria A. Torija was born in Guadalajara, Spain on August 13, 1977. She attended Sagrado Corazon and Salesianos schools, graduating from Salesianos High School in 1995. She passed the Selective Access Exam with 8.33 average, and cursed physics in University of Complutense of Madrid. In 1999-2000, she earned an assitanship in the International Student Program, taking Material and Science Enginnering and graduate physics classes in University of Tennesse Knoxville. In March 2001, she was a scientific visitor Francis Bitter Magntism Lab in Massachusetts Institute of Technology. She finished the Bachelor degrre in Physics in Spain in June of 2001, earning the Cum Laude in Reasearch Final Proyect. Since August 2001, she has been a graduate student in University of Tennesse, Knoxville. After her graduation, she plans to work in the University of Minnesota as postdoctoral associated.